

Adding space to FMD and AI models

Julien Arino

April 2023

Why it is important to incorporate space

General considerations about space-and-time spread

Spatial aspects in animal diseases

Foot-and-mouth disease

Avian influenza

Metapopulation models

A few foot-and-mouth disease models

A few avian influenza models

Why it is important to incorporate space

General considerations about space-and-time spread

Spatial aspects in animal diseases

Foot-and-mouth disease

Avian influenza

Metapopulation models

A few foot-and-mouth disease models

A few avian influenza models

Diseases have been known to be mobile for a while

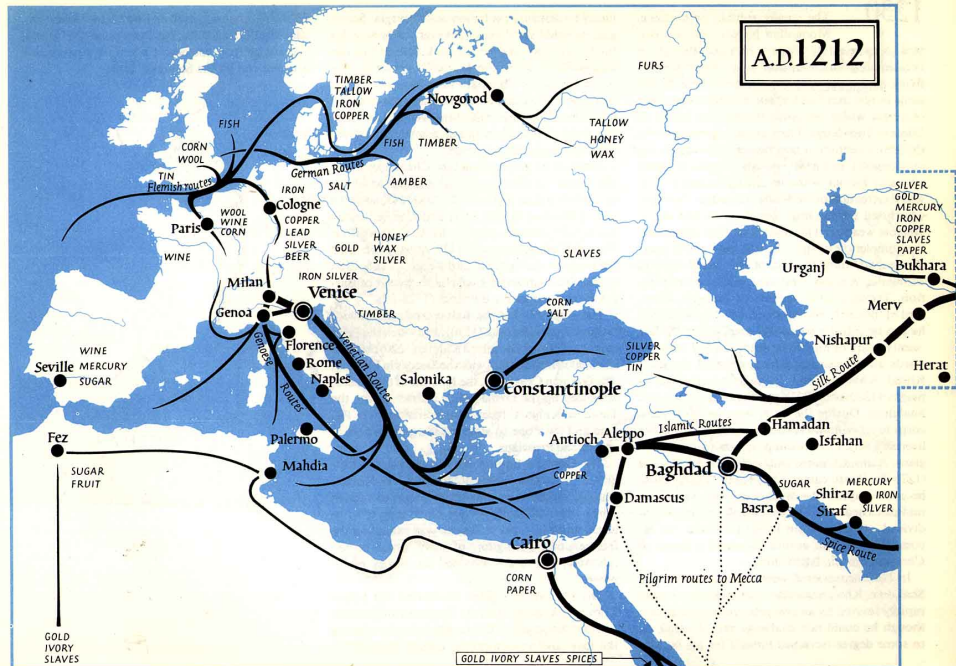
The plague of Athens of 430 BCE

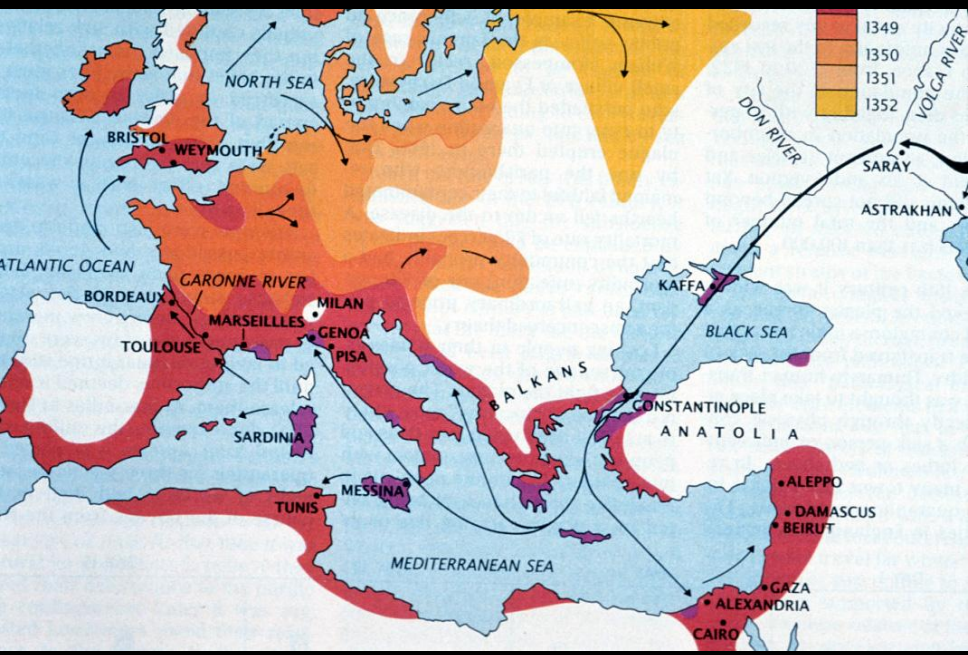
It first began, it is said, in the parts of Ethiopia above Egypt, and thence descended into Egypt and Libya and into most of the [Persian] King's country. Suddenly falling upon Athens, it first attacked the population in Piraeus [...] and afterwards appeared in the upper city, when the deaths became much more frequent.

Thucydides (c. 460 BCE - c. 395 BCE)
History of the Peloponnesian War



A.D 1212

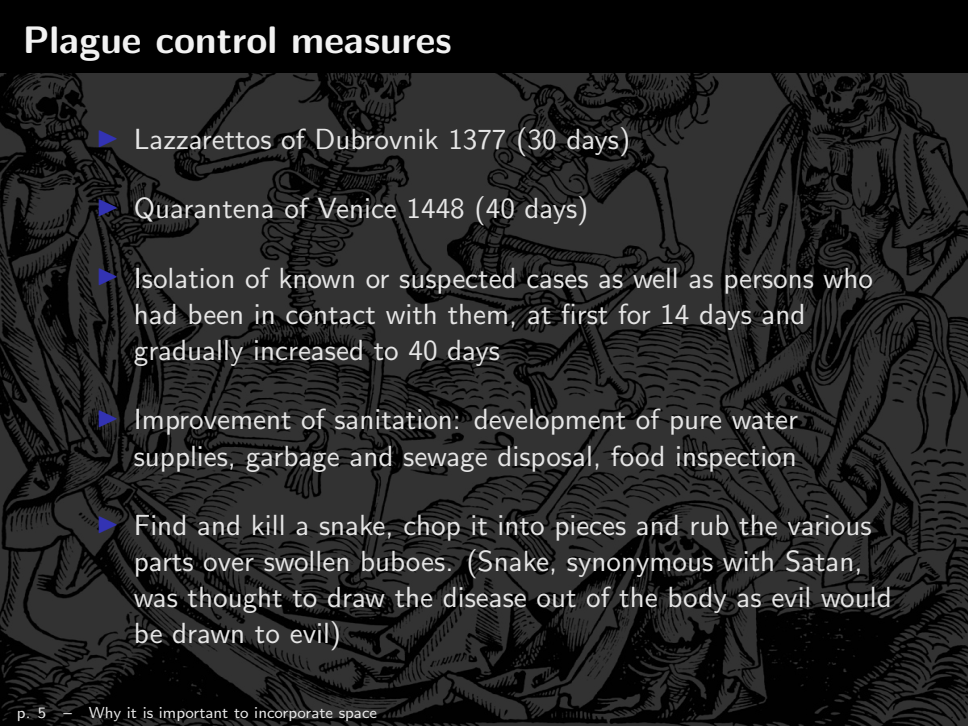




The Black Death: a few facts

- ▶ First of the middle ages plagues to hit Europe
- ▶ Affected Afro-Eurasia from 1346 to 1353
- ▶ Europe 1347-1351
- ▶ Killed 75-200M in Eurasia & North Africa
- ▶ Killed 30-60% of European population

Plague control measures

- 
- ▶ Lazzarettos of Dubrovnik 1377 (30 days)
 - ▶ Quarantena of Venice 1448 (40 days)
 - ▶ Isolation of known or suspected cases as well as persons who had been in contact with them, at first for 14 days and gradually increased to 40 days
 - ▶ Improvement of sanitation: development of pure water supplies, garbage and sewage disposal, food inspection
 - ▶ Find and kill a snake, chop it into pieces and rub the various parts over swollen buboes. (Snake, synonymous with Satan, was thought to draw the disease out of the body as evil would be drawn to evil)

50 0 50 100 150 200
Yards

X Pump

• Deaths from cholera

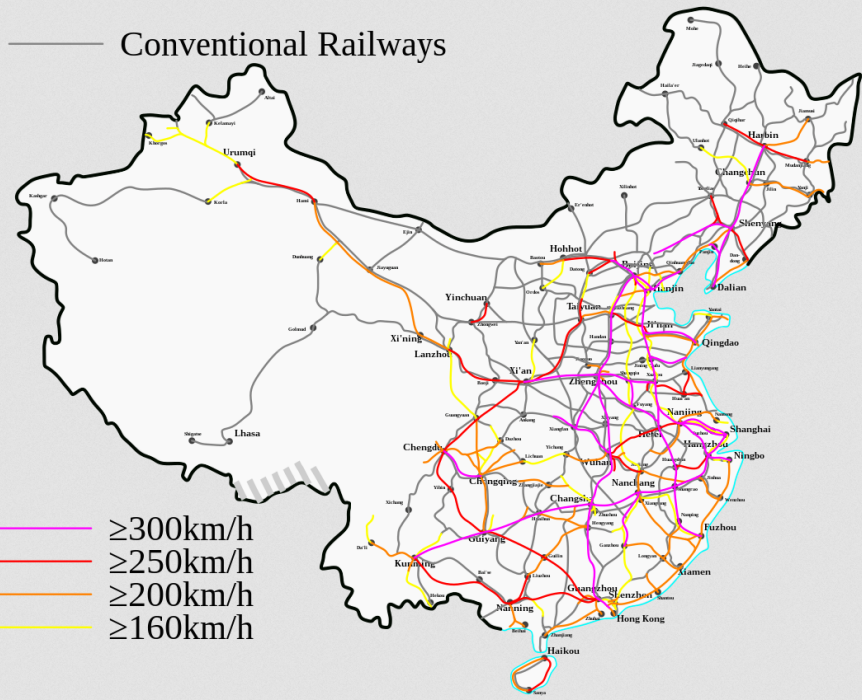


Pathogen spread has evolved with mobility

- ▶ Pathogens travel along trade routes
- ▶ In ancient times, trade routes were relatively easy to comprehend
- ▶ With acceleration and globalization of mobility, things have changed



Conventional Railways



Fragmented jurisdictional landscapes

- ▶ Political divisions (jurisdictions): nation groups (e.g., EU), nations, provinces/states, regions, counties, cities..
- ▶ Travel between jurisdictions can be complicated or impossible
- ▶ Data is integrated at the jurisdictional level
- ▶ Policy is decided at the jurisdictional level

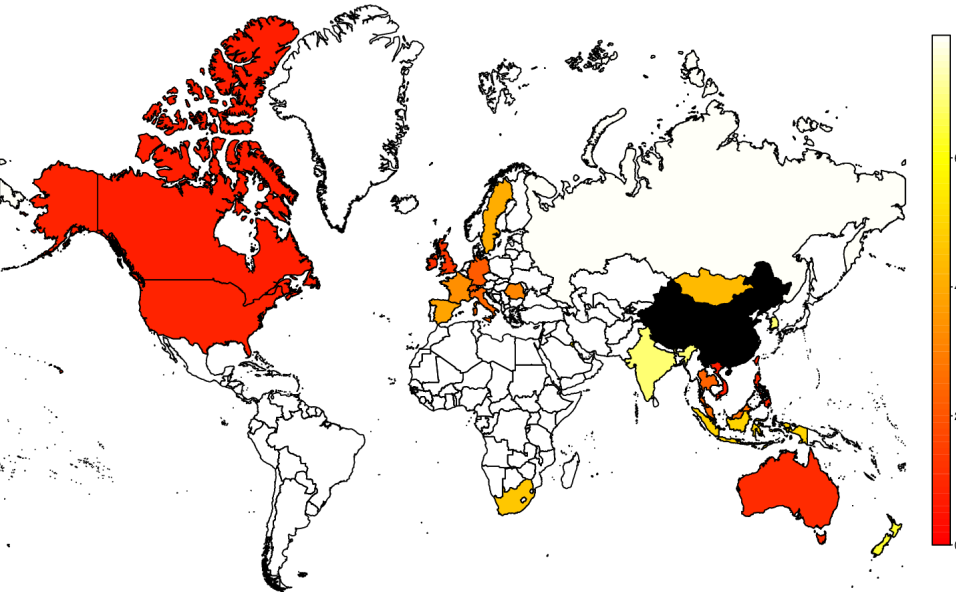
Why mobility is important in the context of health

All migrants/travellers carry with them their "health history"

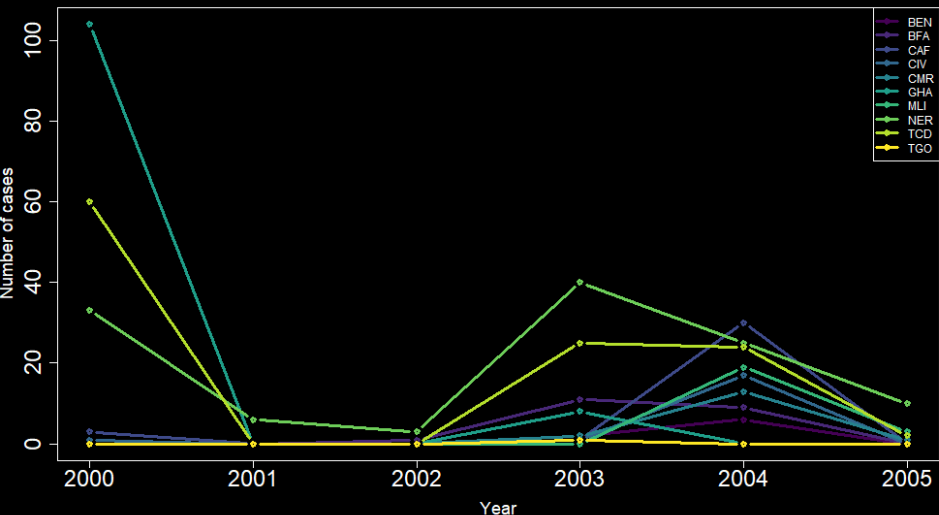
- ▶ latent and/or active infections (TB, H1N1, polio)
- ▶ immunizations (schedules vary by country)
- ▶ health/nutrition practices (KJv)
- ▶ treatment methods (antivirals)

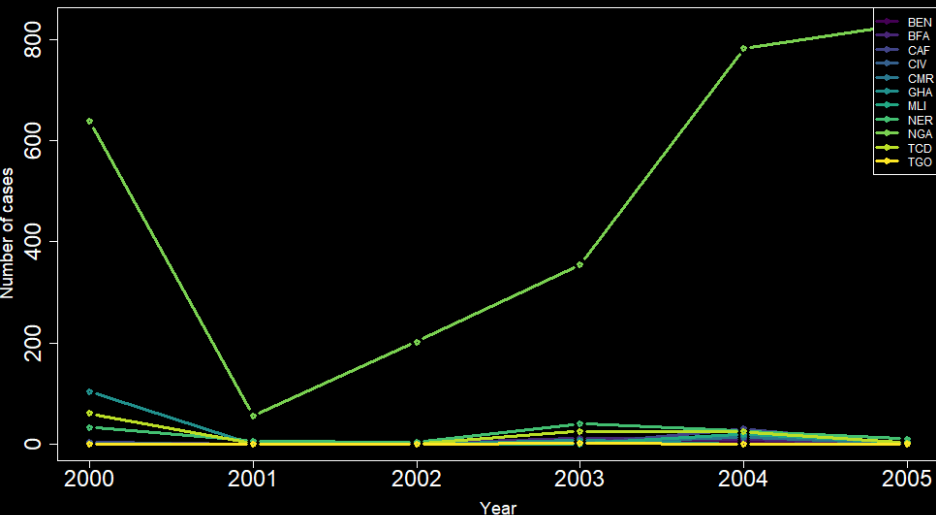
Pathogens ignore borders and politics

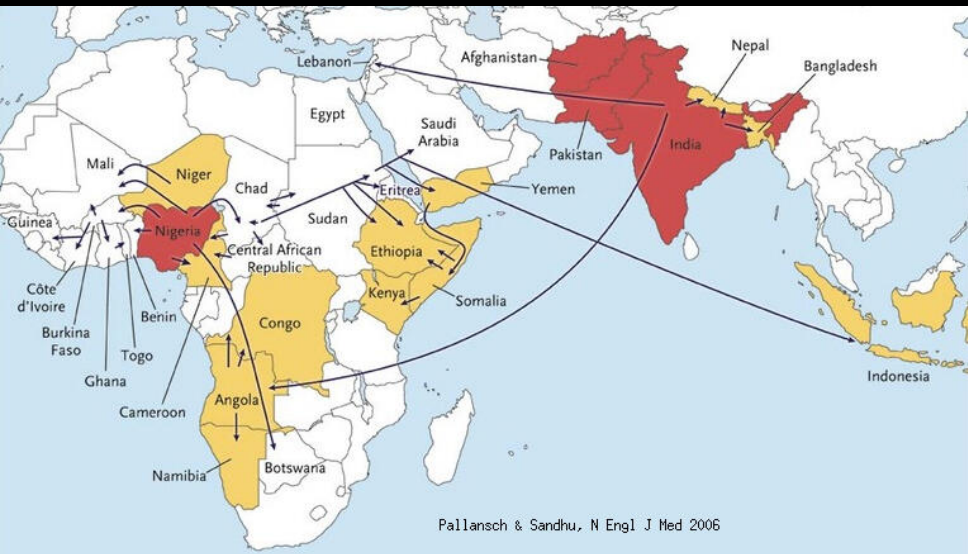
Countries with SARS cases (WHO/Dec 2003)











Pallansch & Sandhu, N Engl J Med 2006

Why it is important to incorporate space

General considerations about space-and-time spread

Spatial aspects in animal diseases

Foot-and-mouth disease

Avian influenza

Metapopulation models

A few foot-and-mouth disease models

A few avian influenza models

Diseases in wild animals

Spread typically follows travelling wave patterns

Next slides: cases of rabies

1990



2000



2010



Diseases in livestock

Situation is more complicated

Why it is important to incorporate space

General considerations about space-and-time spread

Spatial aspects in animal diseases

Foot-and-mouth disease

Avian influenza

Metapopulation models

A few foot-and-mouth disease models

A few avian influenza models

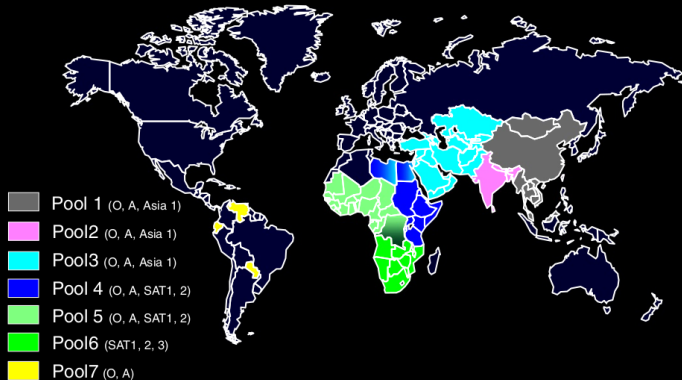


Figure 2 Geographical distribution of seven pools of foot-and-mouth disease viruses. Serotype O FMDV is the most widely distributed serotype of the virus (in 6 of the 7 indicated virus pools) whereas, in contrast, SAT3 is only present in pool 6 (within southern Africa). The Asia-1, SAT1 and SAT2 serotypes also have quite limited geographical distribution. However, individual countries can have multiple serotypes in circulation at the same time and hence it is necessary to be able to determine which serotype is responsible for an outbreak if vaccination is to be used. Countries which are normally free of the disease (marked in yellow) can still suffer incursions of the virus which can have high economic costs.

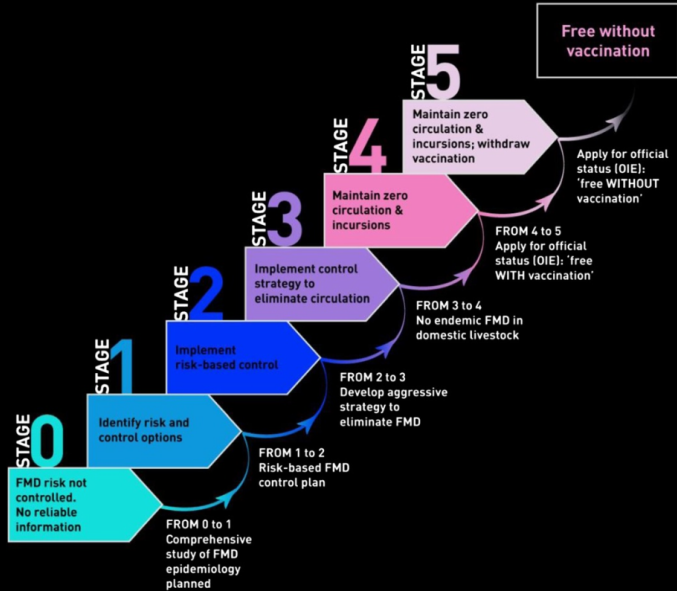


Figure 3 The FAO/EuFMD/OIE Progressive Control Pathway for FMD. The status of countries on the PCP-FMD is evaluated according to defined criteria. Countries with endemic disease are in stages 0 to 3 while countries with no endemic disease within livestock are at stage 4 or above. The image was kindly supplied by EuFMD.

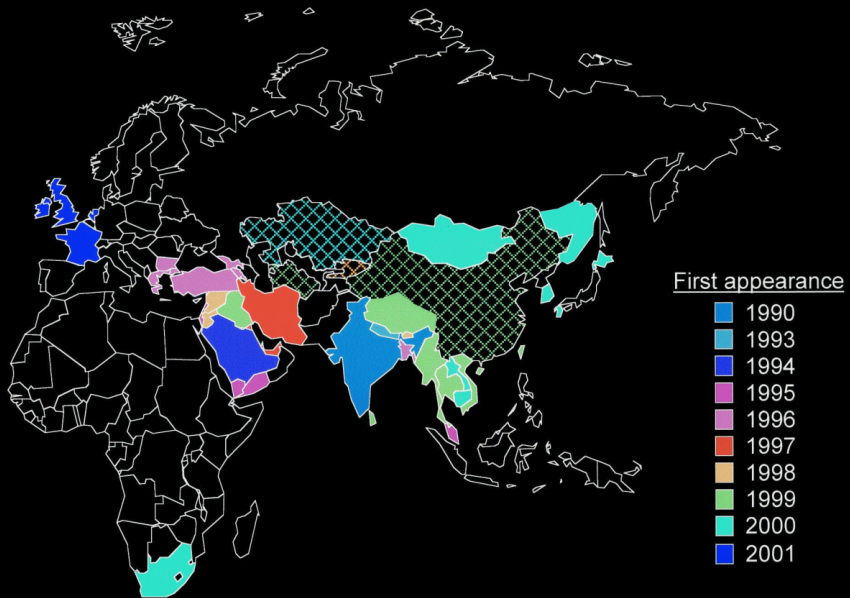


FIG. 4. The spread of the PanAsian strain of FMDV type O from its first appearance in India in 1990 until its appearance in the United Kingdom in 2001. Solid colors, PanAsian strain present; cross-hatched colors, type O present and PanAsian strain suspected. The data and map were compiled by Nick Knowles and can be found at www.iah.bbsrc.ac.uk/virus/picornaviridae/aphthovirus.

Spread of FMD in the old world



Source: WRL at IAH, Pirbright, UK

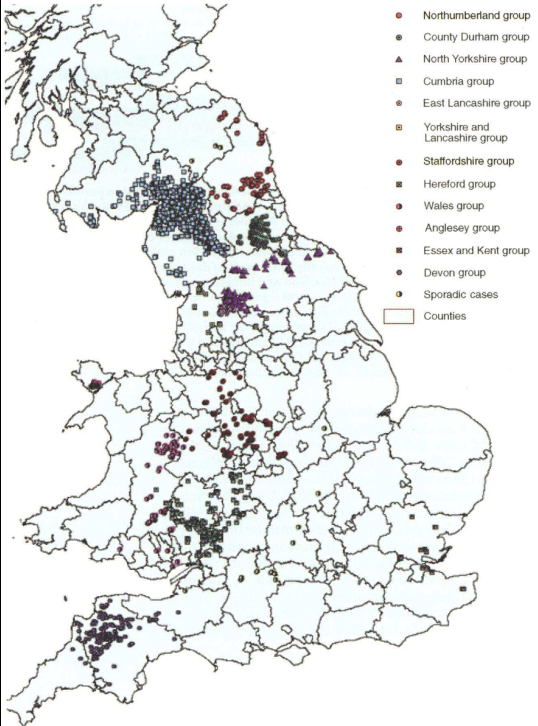
Descriptive epidemiology of the 2001 foot-and-mouth disease epidemic in Great Britain: the first five months

**J. C. GIBBENS, C. E. SHARPE, J. W. WILESMITH, L. M. MANSLEY, E. MICHALOPOULOU,
J. B. M. RYAN, M. HUDSON**

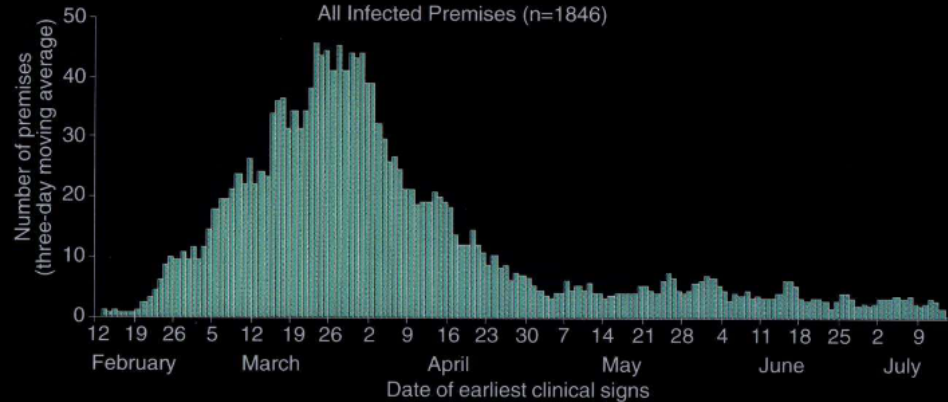
In February 2001, foot-and-mouth disease (FMD) was confirmed in Great Britain. A major epidemic developed, which peaked around 50 cases a day in late March, declining to under 10 a day by May. By mid-July, 1849 cases had been detected. The main control measures employed were livestock movement restrictions and the rapid slaughter of infected and exposed livestock. The first detected case was in south-east England; infection was traced to a farm in north-east England to which all other cases were linked. The epidemic was large as a result of a combination of events, including a delay in the diagnosis of the index case, the movement of infected sheep to market before FMD was first diagnosed, and the time of year. Virus was introduced at a time when there were many sheep movements around the country and weather conditions supported survival of the virus. The consequence was multiple, effectively primary, introductions of FMD virus into major sheep-keeping areas. Subsequent local spread from these introductions accounted for the majority of cases. The largest local epidemics were in areas with dense sheep populations and livestock dealers who were active during the key period. Most affected farms kept both sheep and cattle. At the time of writing the epidemic was still ongoing; however, this paper provides a basis for scientific discussion of the first five months.

Veterinary Record (2001)
149, 729-743

J. C. Gibbens, BVetMed,
MSc, MSc, MRCVS,
J. W. Wilesmith, BVSc,
MRCVS, HonMFPHM, State
Veterinary Service,
DEFRA, 1A Page Street,
London SW1P 4PQ
C. E. Sharpe, BVetMed,
MSc, MRCVS, State



All Infected Premises (n=1846)



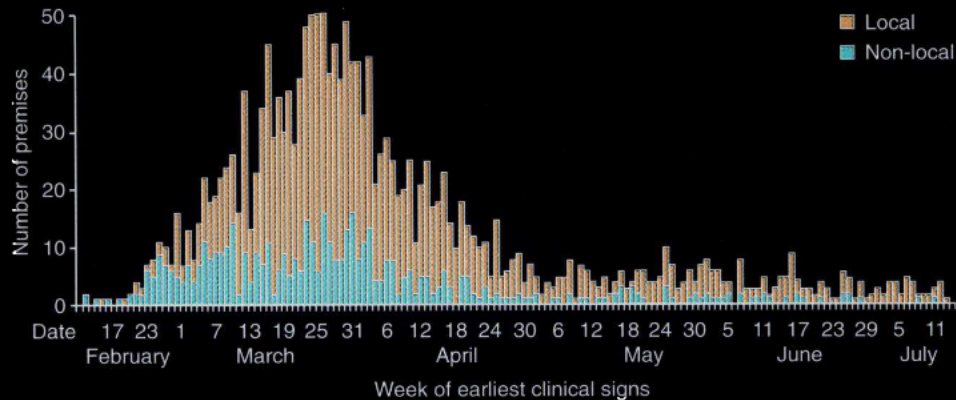


FIG 5: Epidemic curve to show number of foot-and-mouth disease infected premises with early disease each day, categorised to differentiate those within 3 km of an earlier case (local cases). (n=1847, Infected Premises with missing data excluded)

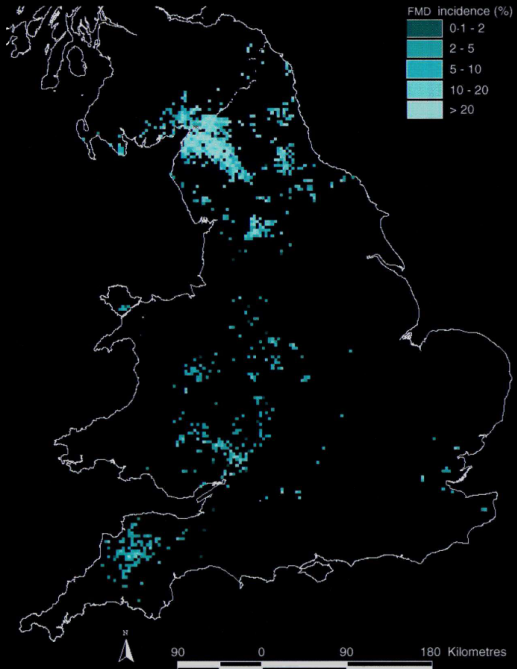


FIG 9: Cumulative incidence of foot-and-mouth disease (FMD) in Great Britain, February 10 to July 15, 2001

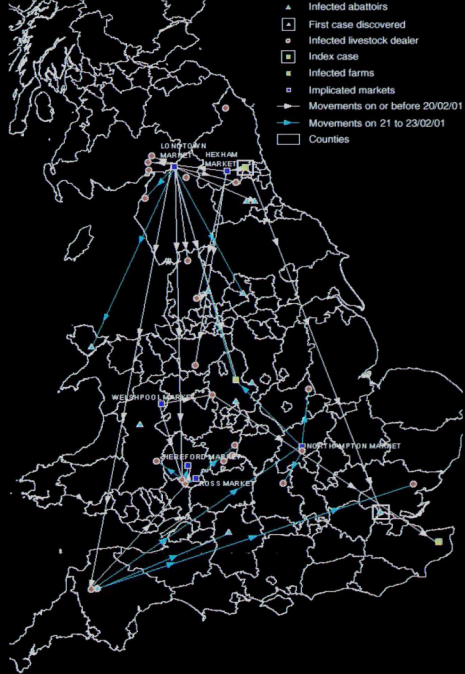


FIG 3: Movement of foot-and-mouth disease infected animals before February 23, 2001,
and location of implicated markets, abattoirs and dealers (subject to information
available on August 30, 2001)

2001 FMD epidemic in the UK

- ▶ Early February – Disease likely to have entered the UK
- ▶ 19th February – Foot-and-mouth disease first suspected
- ▶ 20th February – Foot-and-mouth disease confirmed
- ▶ 23rd February – Culling initiated of Infected Premises (IP) and Dangerous Contacts (DC). Movement restrictions are brought into force
- ▶ 15th March – Sheep, goats and pigs within 3km of an IP in Lockerbie, Carlisle and Solway are targeted for culling
- ▶ 23rd March – Contiguous Premises (CPs) are included in the cull
- ▶ 26th March – Epidemic reaches its maximum with 54 cases in one day
- ▶ 27th March – 3km cull begins in the Penrith valley, Cumbria
- ▶ 29th March – 24/48 hour policy begins, in which IPs are slaughtered within 24 hours, and DCs and CPs are culled within 48 hours
- ▶ 14th April – 3km cull in Cumbria reaches its height
- ▶ 26th April – Sheep, pigs and especially cattle from farms with high biosecurity may be exempt from culls
- ▶ 10th May – First case reported in the Settle area
- ▶ 20th June – First day with no reported cases

Why it is important to incorporate space

General considerations about space-and-time spread

Spatial aspects in animal diseases

Foot-and-mouth disease

Avian influenza

Metapopulation models

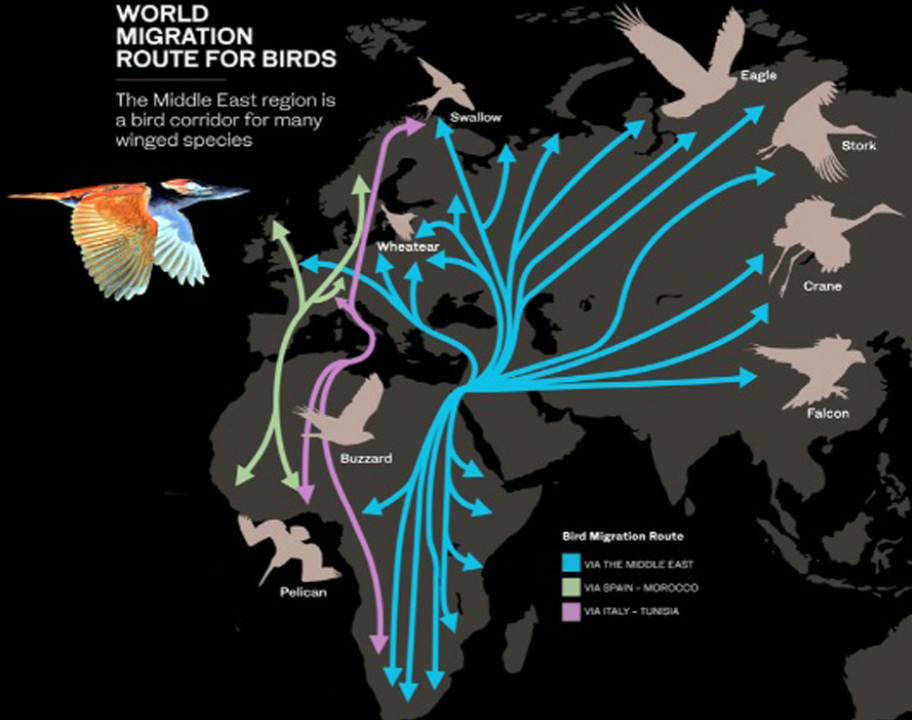
A few foot-and-mouth disease models

A few avian influenza models

- ▶ Avian Influenza global concern because it involves multiple bird species, both wild and livestock
- ▶ The thing with wild birds is that they fly... :)

WORLD MIGRATION ROUTE FOR BIRDS

The Middle East region is a bird corridor for many winged species



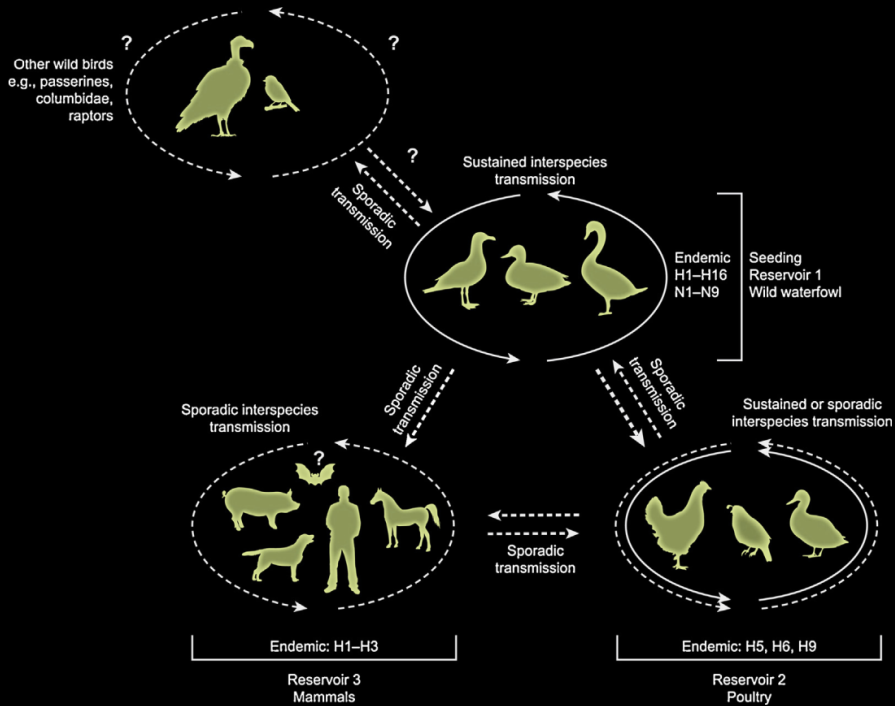


Table 1

Major events in the history of avian influenza

Year	Event	Reference
1878	First description of highly pathogenic avian influenza (HPAI) or fowl plague	[1]
1880	Differentiation of HPAI from fowl cholera	[2]
1901	Identification of HPAI as a virus	[3]
1901–1930s	Major outbreaks of HPAI throughout the world	[6,7,10]
1918	Major human pandemic	[72]
1931	First influenza virus isolated (swine)	[73]
1941	Recognition of hemagglutination by influenza viruses	[16]
1942	HPAI and Newcastle disease virus shown to agglutinate red blood cells and to be different serologically	[17]
1955	HPAI virus shown to be a type A influenza virus	[4]
1959	Isolation of a HPAI virus serologically different from the classical fowl plague virus in hemagglutination inhibition test	[25]
1970s	Intensive surveillance of influenza viruses in wild birds and recognition that wild birds harbor all identified subtypes of influenza viruses	[30–34,37]
1971	Classification of influenza viruses based on antigenic properties of the NP (type) and HA and NA (subtype) proteins and the species of origin	[39]
1977–1981	Recognition that the presence of multiple basic amino acids in the HA cleavage site correlates with tissue spread and virulence of AI strains	[74,75]
1978	Recognition that the 1957 (H2N2) and 1968 (H3N2) pandemic influenza viruses aroused by reassortment with AI viruses	[76]
1980	Classification of influenza viruses based on antigenic properties of the NP (type) and HA and NA (subtype) proteins regardless of the species of origin	[39]
1981	First International Symposium on Avian Influenza	[5]
1981	The name highly pathogenic avian influenza is proposed to substitute fowl plague	[5]
1999–2001	H9N2 virus transmission to humans	[64–67]
1997–present	HPAI H5N1 transmission to humans	This issue
2000s	H9N2 becomes endemic in Asia	[63]
2003–present	HPAI H5N1 spreads through Asia, Europe and Africa and becomes endemic in Asia	This issue

Predicting the global spread of H5N1 avian influenza

A. Marm Kilpatrick^{*†}, Aleksei A. Chmura^{*}, David W. Gibbons[‡], Robert C. Fleischer[§], Peter P. Marra[¶], and Peter Daszak^{*}

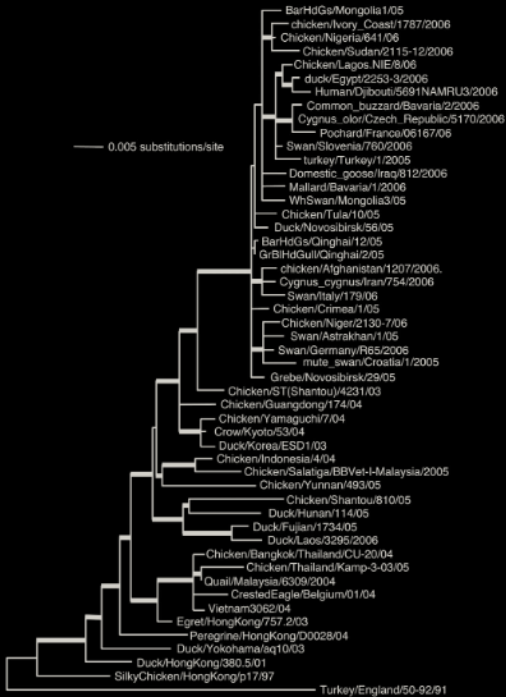
^{*}Consortium for Conservation Medicine, New York, NY 10001; [†]Royal Society for the Protection of Birds, Sandy, Bedfordshire SG19 2DL, United Kingdom; and [§]National Museum of Natural History, and [¶]Smithsonian Migratory Bird Center, National Zoological Park, Smithsonian Institution, Washington, DC 20008

Communicated by Hans R. Herren, Millennium Institute, Arlington, VA, October 19, 2006 (received for review April 26, 2006)

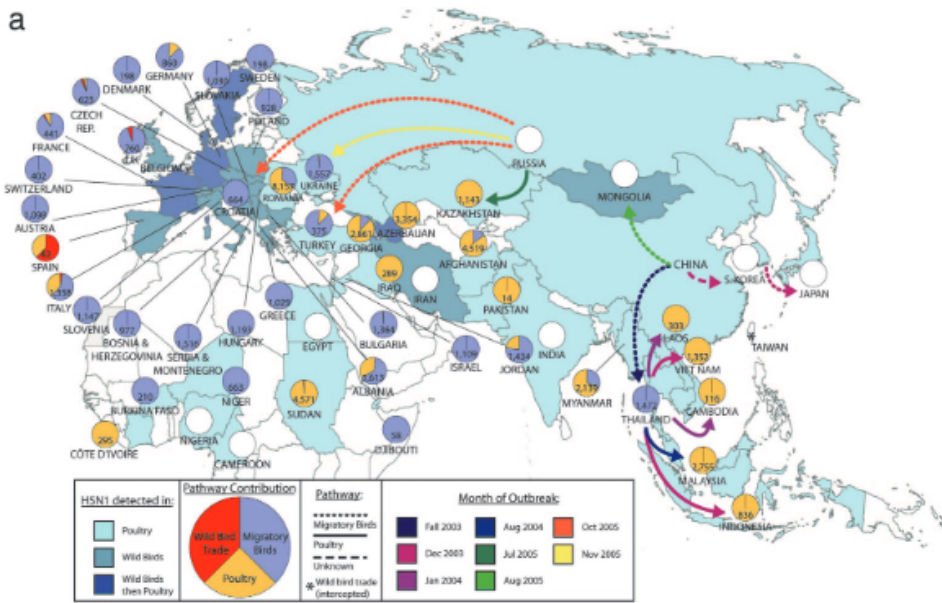
The spread of highly pathogenic H5N1 avian influenza into Asia, Europe, and Africa has resulted in enormous impacts on the poultry industry and presents an important threat to human health. The pathways by which the virus has and will spread between coun-

commercial trade in wild birds (4), making this another potentially important pathway unless all imported birds are quarantined, tested for avian influenza, and culled where necessary.

We determined the most likely pathways for the introduction



a



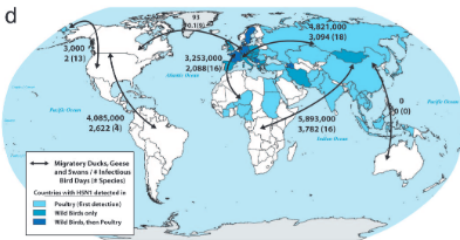
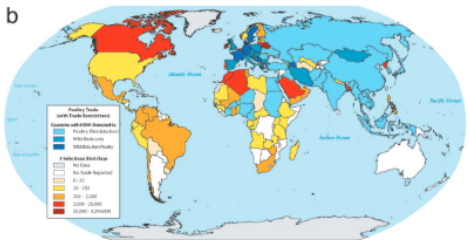
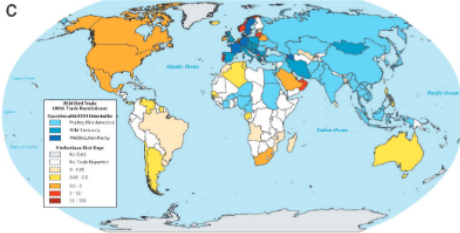
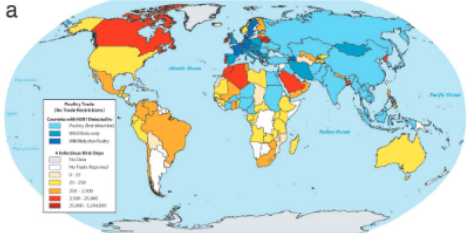


Fig. 2. Predicted risk of H5N1 avian influenza introduction from countries that have had H5N1 outbreaks (in blue). (a–c) Risk was estimated as the number of infectious bird days (number of infected birds × days shedding virus) caused by trade (presented as yearly totals/12 months) in: live poultry with no trade restrictions (a), live poultry with no exports from countries reporting H5N1 in poultry (France, Denmark, Sweden, and Germany are considered H5N1-free) (b), and captive wild birds with no exports from countries reporting H5N1 in poultry (c) as in b. (d) Estimated number of ducks, geese, and swans migrating between mainland continents, number of infectious bird days, and number of species (in parentheses). Numbers given between Asia and North America include only those that breed on mainland Asia and winter in North America south of Alaska; an additional 200,000–400,000 ducks breed in Siberia and molt or winter in or off the coast of Alaska. In addition, ~20,000 geese migrate between Ireland and North America.

Emergence and spread of highly pathogenic avian influenza A(H5N8) in Europe in 2016-2017

S. Napp¹  | N. Majó² | R. Sánchez-González¹ | J. Vergara-Alert¹

¹Institut de Recerca i Tecnologia Agroalimentàries (IRTA), Bellaterra, Barcelona, Spain

²Universitat Autònoma de Barcelona, Bellaterra, Barcelona, Spain

Correspondence

S. Napp, IRTA, Centre de Recerca en Sanitat Animal (CReSA), Campus de la Universitat Autònoma de Barcelona, Bellaterra (Cerdanyola del Vallès), Spain.
Email: sebastian.napp@irta.es

Summary

Circulation of highly pathogenic avian influenza (HPAI) viruses poses a continuous threat to animal and public health. After the 2005–2006 H5N1 and the 2014–2015 H5N8 epidemics, another H5N8 is currently affecting Europe. Up to August 2017, 1,112 outbreaks in domestic and 955 in wild birds in 30 European countries have been reported, the largest epidemic by a HPAI virus in the continent. Here, the main epidemiological findings are described. While some similarities with previous HPAI virus epidemics were observed, for example in the pattern of emergence, significant differences were also patent, in particular the size and extent of the epidemic. Even though no human infections have been reported to date, the fact that A/H5N8 has affected so far 1,112 domestic holdings, increases the risk of exposure of humans and therefore represents a concern. Understanding the epidemiology of HPAI viruses is essential for the planning future surveillance and control activities.

KEY WORDS

domestic birds, epidemiology, H5N8, highly pathogenic avian influenza virus, wild birds

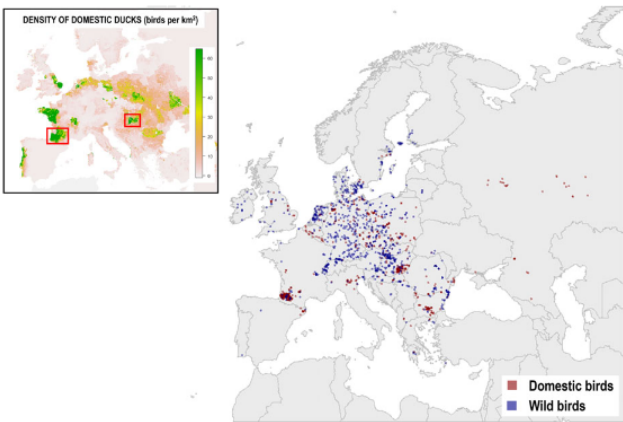


FIGURE 1 Spatial distribution of outbreaks of H5N8 HPAI in domestic (red dots) and wild (blue dots) birds in Europe. Box in the upper left corner represents the density of domestic ducks (birds per km²) in Europe (from Robinson et al., 2014). Red squares mark the areas of high density of ducks in France and Hungary, where clustering of H5N8 outbreaks in poultry occurred [Colour figure can be viewed at wileyonlinelibrary.com]

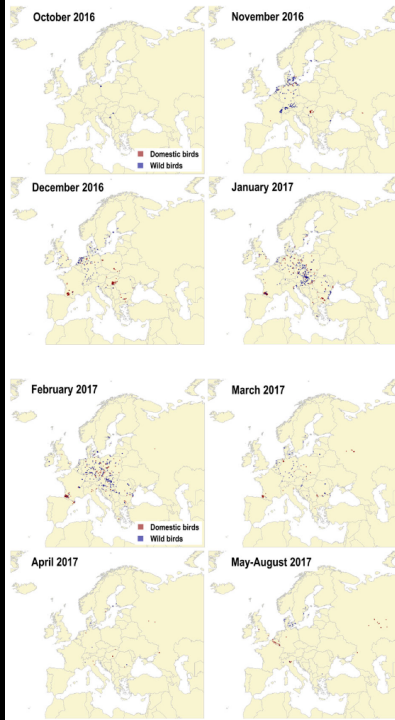


TABLE 1 Outbreaks of H5N8 detected in both domestic and wild birds in Europe between June, 2016 and August 2017, as well as the month and year of onset of outbreaks in domestic and wild, and whether this first onset occurred in domestic or wild birds (the term same is used when domestic and wild outbreaks occurred within the same week)

Country	Domestic birds	Wild birds	Total	Onset domestic	Onset wild	First onset
Austria	2	24	26	November 2016	November 2016	Same
Belgium	13	4	17	June 2017	February 2017	Wild
Bosnia	1	2	3	February 2017	February 2017	Domestic
Bulgaria	67	13	80	December 2016	December 2016	Domestic
Croatia	7	11	18	December 2016	October 2016	Wild
Czech Republic	43	40	83	January 2017	January 2017	Same
Denmark	2	51	53	November 2016	November 2016	Wild
Finland	0	15	15		November 2016	Wild
France	420	55	475	December 2016	November 2016	Wild
Germany	94	194	288	November 2016	November 2016	Same
Greece	7	8	15	January 2017	December 2016	Wild
Hungary	239	54	293	November 2016	October 2016	Wild
Ireland	0	10	10		December 2016	Wild
Italy	20	8	28	January 2017	December 2016	Wild
Lithuania	0	5	5		February 2017	Wild
Luxembourg	4		4	June 2017		Domestic
Netherlands	9	56	65	November 2016	November 2016	Wild
Macedonia	2		2	January 2017		Domestic
Poland	65	69	134	December 2016	October 2016	Wild
Portugal	0	1	1		January 2017	Wild
Romania	44	90	134	December 2016	November 2016	Wild
Russia	27	1	28	November 2016	June, 2016	Wild
Serbia	4	13	17	January 2017	December 2016	Wild
Slovakia	10	63	73	December 2016	January 2017	Domestic
Slovenia	0	20	20		January 2017	Wild
Spain	10	2	12	February 2017	January 2017	Wild
Sweden	6	37	43	November 2016	November 2016	Same
Switzerland	0	87	87		November 2016	Wild
UK	13	19	32	December 2016	December 2016	Same
Ukraine	3	3	6	December 2016	January 2017	Domestic
Total	1,112	955	2,067			

TABLE 2 Number and percentage of domestic outbreaks affected by the H5N8 according to the size of the holding for different European countries

	Size of domestic holdings affected according to the number of birds				
	100	500	1,000	10,000	>10,000
	<100	500	1,000	10,000	>10,000
Czech Republic	30 (70%)	6 (14%)	2 (5%)	2 (5%)	3 (7%)
France	183 (46%)	8 (2%)	27 (7%)	140 (35%)	40 (10%)
Germany	20 (22%)	8 (9%)	0 (0%)	23 (25%)	41 (45%)
Hungary	15 (7%)	24 (10%)	10 (4%)	100 (44%)	80 (35%)
Poland	21 (33%)	5 (8%)	2 (3%)	8 (13%)	28 (44%)
Romania	38 (86%)	6 (14%)	0 (0%)	0 (0%)	0 (0%)
Total Europe	375 (37%)	82 (8%)	43 (4%)	283 (28%)	229 (23%)

Role for migratory wild birds in the global spread of avian influenza H5N8

The Global Consortium for H5N8 and Related Influenza Viruses*†

Avian influenza viruses affect both poultry production and public health. A subtype H5N8 (clade 2.3.4.4) virus, following an outbreak in poultry in South Korea in January 2014, rapidly spread worldwide in 2014–2015. Our analysis of H5N8 viral sequences, epidemiological investigations, waterfowl migration, and poultry trade showed that long-distance migratory birds can play a major role in the global spread of avian influenza viruses. Further, we found that the hemagglutinin of clade 2.3.4.4 virus was remarkably promiscuous, creating reassortants with multiple neuraminidase subtypes. Improving our understanding of the circumpolar circulation of avian influenza viruses in migratory waterfowl will help to provide early warning of threats from avian influenza to poultry, and potentially human, health.

In 2014, highly pathogenic avian influenza (HPAI) virus of the subtype H5N8 caused disease outbreaks in poultry in Asia, Europe, and North America (1–3). Avian influenza viruses are a threat both to global poultry production and to public health; they have the potential to cause severe disease in people and to adapt to transmit efficiently in human populations (4). This was the first time since 2005 that a single subtype of HPAI virus had spread over such a large geographical area and the first time that a Eurasian HPAI virus had spread to

North America. The rapid global spread of HPAI H5N8 virus outbreaks raised the question of the routes by which the virus had been transmitted.

The segment encoding for the hemagglutinin (HA) surface protein of the HPAI H5N8 viruses is a descendant of the HPAI H5N1 virus (A/Goose/Guangdong/1/1996), first detected in China in 1996 (5). Since then, HPAI H5N1 viruses have become endemic in poultry populations in several countries. The H5 viruses have developed new characteristics by mutation and by reassortment with other avian influenza (AI) viruses, both in poultry and in wild birds. In 2005–2006, HPAI H5N1 spread from Asia to Europe, the Middle East, and Africa during the course of a few months. Although virus spread traditionally had been

*Corresponding author. Email: lkuiken@erasmusmc.nl †All authors with their affiliations appear at the end of this paper.

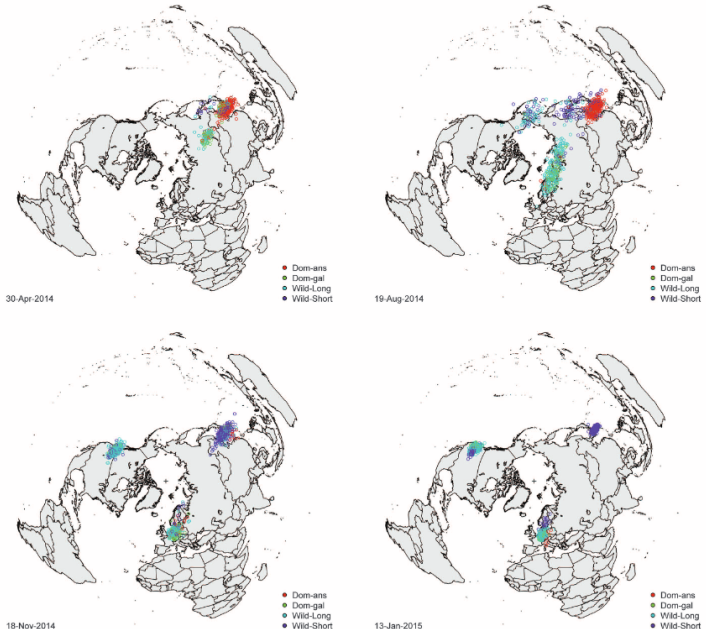


Fig. 2. Reconstruction of the transmission routes using phylogenetic data only from H5N8 HA sequences. At each time slice, the host type and location coordinates on the branches of the posterior set of phylogenetic trees are inferred and plotted as a cloud of points. The host type was inferred by discrete trait model (as Fig. 1) (14), and the continuous location coordinates were inferred using a homogeneous Brownian motion diffusion model (15). The map projection used is the azimuthal equal areas projection, centered on the North Pole, which is marked with a + sign. Color key as for Fig. 1; see also movie S1.

Why it is important to incorporate space

Metapopulation models

Metapopulations à la Levins

Metapopulations à la Levin

The graph setting

Generic model

The movement matrix

Behaviour of the mobility component

A few sample models

Existence of a DFE

Computation of a reproduction number

Computational considerations

A few foot-and-mouth disease models

A few avian influenza models

What are metapopulations?

Metapopulations are *populations of populations*.

Two main types of metapopulation models:

- ▶ *patch occupancy models.* Describe whether a location is *occupied* by a species or not. Depends on the occupancy of neighboring or connected locations. Dynamics describes the number of occupied locations
- ▶ Models with *explicit movement*. Movement between locations is described explicitly. In each location, a set of differential equations describes the dynamics of the populations present

What is a location?



A *location* is a unit (typically geographical) within which the population is considered homogeneous

- ▶ city
- ▶ region
- ▶ country
- ▶ but also, location where a given species lives (for example, forest, swamp, etc.)

Locations may or may not overlap

Why it is important to incorporate space

Metapopulation models

Metapopulations à la Levins

Metapopulations à la Levin

The graph setting

Generic model

The movement matrix

Behaviour of the mobility component

A few sample models

Existence of a DFE

Computation of a reproduction number

Computational considerations

A few foot-and-mouth disease models

A few avian influenza models

A model of Richard Levins (1969)

R. Levins. Some Demographic and Genetic Consequences of Environmental Heterogeneity for Biological Control. Bulletin of the Entomological Society of America 15(3): 237-240 (1969)

Cited 4,400+ times, numerous higher order “offspring”

Quickly evolved to include prey-predators or competition systems

The Levins model

Rate of change of # of local populations P :

$$P' = \beta P \left(1 - \frac{P}{T}\right) - \mu P \quad (1)$$

β immigration rate between *locations*, T total number of locations
and μ extinction rate of local populations

Ecologists & mathematicians think of patches differently. For mathematicians, typically, one place in space. To be clear, in the remainder of these slides, I will speak of *locations*

Metapopulations with implicit movement

Same philosophy as the Levins model

- ▶ There is a set \mathcal{P} of locations called *locations*
- ▶ Each location $p \in \mathcal{P}$ has an internal dynamics $x'_p = f_p(x_p)$, where $x_p \in \mathbb{R}_+^{n_p}$ and $f_p : \mathbb{R}^{n_p} \rightarrow \mathbb{R}^{n_p}$
- ▶ No flow of individuals between locations
- ▶ The influence of location $q \neq p$ on p is described through a function $g_{qp}(x_p, x_q)$, where $x_q \in \mathbb{R}^{n_q}$ and $g_p : \mathbb{R}^{n_p} \times \mathbb{R}^{n_q} \rightarrow \mathbb{R}^{n_p}$

So the population in location $p \in \mathcal{P}$ has dynamics

$$x'_p = f_p(x_p) + \sum_{\substack{q \in \mathcal{P} \\ q \neq p}} g_{qp}(x_p, x_q) \quad (2)$$

Why it is important to incorporate space

Metapopulation models

Metapopulations à la Levins

Metapopulations à la Levin

The graph setting

Generic model

The movement matrix

Behaviour of the mobility component

A few sample models

Existence of a DFE

Computation of a reproduction number

Computational considerations

A few foot-and-mouth disease models

A few avian influenza models

Levins-type vs Explicit movement

Levins model and its offspring: movement is implicit

$$P' = \beta P \left(1 - \frac{P}{T} \right) - \mu P$$

β immigration rate between locations incorporates geography

Sometimes we have explicit movement information or want to incorporate known spatial information \implies models with explicit movement

Levin (1974)

Metapopulations with explicit movement

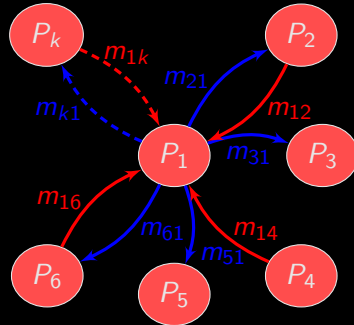
Split continuous space into N discrete geographical locations (*ptatches*)

Each location contains **compartments** (homogeneous groups of individuals). E.g., preys, predators, etc.

Here, we consider a single compartment, the *species of interest*, with no further compartmentalisation

Individuals *may* move between locations; $m_{qp} \geq 0$ rate of movement of individuals from location $p = 1, \dots, N$ to location $q = 1, \dots, N$

Explicit movement (focus on P_1)



$$P'_1 = \sum_{\substack{j=1 \\ j \neq 1}}^N m_{1j} P_j - P_1 \sum_{\substack{j=1 \\ j \neq 1}}^N m_{j1}$$

or

$$P'_1 = \sum_{j=1}^N m_{1j} P_j \text{ assuming } m_{11} = - \sum_{\substack{j=1 \\ j \neq 1}}^N m_{j1}$$

Why it is important to incorporate space

Metapopulation models

Metapopulations à la Levins

Metapopulations à la Levin

The graph setting

Generic model

The movement matrix

Behaviour of the mobility component

A few sample models

Existence of a DFE

Computation of a reproduction number

Computational considerations

A few foot-and-mouth disease models

A few avian influenza models

Graph setting

Suppose

- ▶ $|\mathcal{P}|$ locations, vertices in a (directed) graph \mathcal{G}
- ▶ Each location contains a certain number of compartments belonging to a common set \mathcal{C} of compartments
- ▶ Arcs of \mathcal{G} represent the possibility for a given compartment to move between two locations; any two locations are connected by a maximum of $|\mathcal{C}|$ edges

Graph is a digraph: movement is not always symmetric

$\mathcal{G} = (\mathcal{P}, \mathcal{A})$ is multi-digraph, where

- ▶ \mathcal{P} is the set of vertices (locations)
- ▶ \mathcal{A} is the set of arcs, i.e., an ordered multiset of pairs of elements of \mathcal{P}

Any two vertices $X, Y \in \mathcal{P}$ are connected by at most $|\mathcal{C}|$ arcs from X to Y and at most $|\mathcal{C}|$ arcs from Y to X

Because there are $|\mathcal{C}|$ compartments and movements are compartment-specific, we also define, for all $c \in \mathcal{C}$, \mathcal{P}_c and \mathcal{A}_c as well as the compartment-specific digraphs $\mathcal{G}^c = (\mathcal{P}_c, \mathcal{A}_c)$

Connection matrix

For a given compartment $c \in \mathcal{C}$, a *connection matrix* can be associated to the digraph \mathcal{G}_c

This is the **adjacency matrix** of \mathcal{G}_c , but we emphasize the reason why we use \mathcal{G}_c by using the term *connection*

Choosing an ordering of elements of \mathcal{P} , the (i, j) entry of the $|\mathcal{P}| \times |\mathcal{P}|$ -matrix $\mathcal{N}_c = \mathcal{N}_c(\mathcal{G}_c)$ is one if $R^c(P_i, P_j)$ and zero otherwise, i.e., if P_i has no direct access to P_j

For convenience, the ordering of the locations is generally assumed the same for all compartments

Strongly connected multi-digraph

Definition 1 (Strongly connected components)

For a given compartment s , the **strongly connected components** (or **strong components**, for short) are such that, for all locations X, Y in a strong component, compartment s in X has access to Y

Definition 2 (Strong connectedness for a compartment)

The multi-digraph is strongly connected for compartment c if all locations belong to the same strong component of \mathcal{G}_c

Strong connectedness and irreducibility

Definition 3 (Reducible/irreducible matrix)

A matrix A is **reducible** if there exists a permutation matrix P such that P^TAP is block upper triangular. A matrix that is not reducible is **irreducible**

Matrix $A \in \mathbb{F}^{n \times n}$ is irreducible if for all $i, j = 1, \dots, n$, there exists k such that $a_{ij}^k > 0$, where a_{ij}^k is the (i, j) -entry in A^k

Theorem 4

Strong connectedness \Leftrightarrow irreducibility of the connection matrix \mathcal{C}_c

Why it is important to incorporate space

Metapopulation models

Metapopulations à la Levins

Metapopulations à la Levin

The graph setting

Generic model

The movement matrix

Behaviour of the mobility component

A few sample models

Existence of a DFE

Computation of a reproduction number

Computational considerations

A few foot-and-mouth disease models

A few avian influenza models

Notation

- ▶ $N_{cp}(t)$ number of individuals of compartment c in location p at time t
- ▶ $\mathbf{N}_c = (N_{c1}, \dots, N_{c|\mathcal{P}|})^T$ distribution of individuals of compartment $c \in \mathcal{C}$ among the different locations
- ▶ $\mathbf{N}^p = (N_1^p, \dots, N_{|\mathcal{P}|}^p)^T$ composition of the population in location $p \in \mathcal{P}$

Metapopulation models with linear movement

Use a linear autonomous movement operator

Then, for a given compartment $c \in \mathcal{C}$ and in a given location $p \in \mathcal{P}$

$$N'_{cp} = f_{cp}(N^p) + \sum_{\substack{q \in \mathcal{P} \\ q \neq p}} m_{cpq} N_{cq} - \left(\sum_{\substack{q \in \mathcal{P} \\ q \neq p}} m_{cqp} \right) N_{cp}$$

where m_{cpq} rate of movement of individuals in compartment $c \in \mathcal{C}$ from location $q \in \mathcal{P}$ to location $p \in \mathcal{P}$

A more compact notation

To make

$$N'_{cp} = f_{cp}(N^p) + \sum_{\substack{q \in \mathcal{P} \\ q \neq p}} m_{cpq} N_{cq} - \left(\sum_{\substack{q \in \mathcal{P} \\ q \neq p}} m_{cqp} \right) N_{cp}$$

more compact, denote the rate of leaving location p as

$$m_{cpp} = - \sum_{\substack{q \in \mathcal{P} \\ q \neq p}} m_{cqp} \quad (3)$$

Then

$$N'_s = f_{cp}(N^p) + \sum_{q \in \mathcal{P}} m_{cpq} N_{cq} \quad (4)$$

Vector form of the system

For compartment $c \in \mathcal{C}$,

$$\mathbf{N}'_c = f(\mathbf{N}) + \mathcal{M}_c \mathbf{N}_c \quad (5)$$

with

$$\mathcal{M}_c = \begin{pmatrix} -\sum_{k \in \mathcal{P}} m_{ck1} & m_{c12} & \cdots & m_{c1|\mathcal{P}|} \\ m_{c|\mathcal{P}|1} & m_{c|\mathcal{P}|2} & \cdots & -\sum_{k \in \mathcal{P}} m_{ck|\mathcal{P}|} \end{pmatrix} \quad (6)$$

Why it is important to incorporate space

Metapopulation models

Metapopulations à la Levins

Metapopulations à la Levin

The graph setting

Generic model

The movement matrix

Behaviour of the mobility component

A few sample models

Existence of a DFE

Computation of a reproduction number

Computational considerations

A few foot-and-mouth disease models

A few avian influenza models

Definitions and notation for matrices

- ▶ $M \in \mathbb{R}^{n \times n}$ a square matrix with entries denoted m_{ij}
- ▶ $M \geq \mathbf{0}$ if $m_{ij} \geq 0$ for all i, j (could be the zero matrix); $M > \mathbf{0}$ if $M \geq \mathbf{0}$ and $\exists i, j$ with $m_{ij} > 0$; $M \gg \mathbf{0}$ if $m_{ij} > 0 \quad \forall i, j = 1, \dots, n$. Same notation for vectors
- ▶ $\sigma(M) = \{\lambda \in \mathbb{C}; M\lambda = \lambda\mathbf{v}, \mathbf{v} \neq \mathbf{0}\}$ **spectrum** of M
- ▶ $\rho(M) = \max_{\lambda \in \sigma(M)} \{|\lambda|\}$ **spectral radius**
- ▶ $s(M) = \max_{\lambda \in \sigma(M)} \{\operatorname{Re}(\lambda)\}$ **spectral abscissa** (or **stability modulus**)
- ▶ M is an **M-matrix** if it is a **Z-matrix** ($m_{ij} \leq 0$ for $i \neq j$) and $M = s\mathbb{I} - A$, with $A \geq \mathbf{0}$ and $s \geq \rho(A)$

The movement matrix

The matrix

$$\mathcal{M}_c = \begin{pmatrix} -\sum_{k \in \mathcal{P}} m_{ck1} & m_{c12} & \cdots & m_{c1|\mathcal{P}|} \\ m_{c|\mathcal{P}|1} & m_{c|\mathcal{P}|2} & \cdots & -\sum_{k \in \mathcal{P}} m_{ck|\mathcal{P}|} \end{pmatrix} \quad (6)$$

is the **movement matrix**

It plays an extremely important role in the analysis of metapopulation systems, so we'll spend some time discussing its properties

\mathcal{M}_c describes

- ▶ existence of connections
- ▶ when they exist, their “intensity”

Properties of the movement matrix \mathcal{M}

First, remark $-\mathcal{M}_c$ is a Laplacian matrix

Lemma 5

1. $0 \in \sigma(\mathcal{M})$ corresponding to left e.v. $\mathbb{1}^T$ [σ spectrum]
2. $-\mathcal{M}$ is a singular M-matrix
3. $0 = s(\mathcal{M}) \in \sigma(\mathcal{M})$ [s spectral abscissa]
4. If \mathcal{M} irreducible, then $s(\mathcal{M})$ has multiplicity 1

For complete proof of Lemma 5 and Proposition 6 (next page), see Arino, Bajeux & Kirkland, BMB 2019

Proposition 6 (D a diagonal matrix)

1. $s(\mathcal{M} + d\mathbb{I}) = d, \forall d \in \mathbb{R}$
2. $s(\mathcal{M} + D) \in \sigma(\mathcal{M} + D)$ associated to $\mathbf{v} > \mathbf{0}$. If \mathcal{M} irreducible, $s(\mathcal{M} + D)$ has multiplicity 1 and is associated to $\mathbf{v} \gg \mathbf{0}$
3. If $\text{diag}(D) \gg \mathbf{0}$, then $D - \mathcal{M}$ invertible M-matrix and $(D - \mathcal{M})^{-1} > \mathbf{0}$
4. \mathcal{M} irreducible and $\text{diag}(D) > \mathbf{0} \implies D - \mathcal{M}$ nonsingular irreducible M-matrix and $(D - \mathcal{M})^{-1} \gg \mathbf{0}$

Why it is important to incorporate space

Metapopulation models

Metapopulations à la Levins

Metapopulations à la Levin

The graph setting

Generic model

The movement matrix

Behaviour of the mobility component

A few sample models

Existence of a DFE

Computation of a reproduction number

Computational considerations

A few foot-and-mouth disease models

A few avian influenza models

Behaviour of the mobility component

Assume no within-location dynamics, just movement. Then (5) takes the form

$$\mathbf{N}'_c = \mathcal{M}_c \mathbf{N}_c \quad (7)$$

Theorem 7

For a given compartment $c \in \mathcal{C}$, suppose that the movement matrix \mathcal{M}_c is irreducible. Then for any $\mathbf{N}_c(0) > 0$, (7) satisfies

$$\lim_{t \rightarrow \infty} \mathbf{N}_c(t) = \mathbf{N}_c^* \gg 0$$

Note that \mathbf{N}_c^* depends on $\mathbb{1}^T \mathbf{N}_c(0)$

Reduction to total population per location

Let

$$T_p = \sum_{c \in \mathcal{C}} N_{cp}$$

be the total population in location p

It is often possible to obtain, in each location $p \in \mathcal{P}$, an equation for the evolution of the total population that takes the form

$$T'_p = D_p(T_p) + \sum_{c \in \mathcal{C}} \sum_{q \in \mathcal{P}} m_{cpq} N_{cq} \quad (8)$$

where $D_p(T_p)$ describes the demography in location p

Nature of the demography

Most common types of demographic functions

- ▶ $D_p(T_p) = b_p - d_p T_p$ (asymptotically constant population)
- ▶ $D_p(T_p) = b_p T_p - d_p T_p$
- ▶ $D_p(T_p) = d_p T_p - b_p T_p = 0$ (constant population)
- ▶ $D_p(T_p) = r_p T_p(1 - T_p/K_p)$ (logistic demography)

In what follows, assume

$$D_p(T_p) = b_p - d_p T_p \tag{9}$$

Vector / matrix form of the equation

Assuming demography is of the form (9), write (8) in vector form

$$\mathbf{T}' = \mathbf{b} - \mathbf{dT} + \sum_{c \in \mathcal{C}} \mathcal{M}_c \mathbf{N}_c \quad (10)$$

where

- ▶ $\mathbf{b} = (b_1, \dots, b_{|\mathcal{P}|})^T \in \mathbb{R}^{|\mathcal{P}|}$
- ▶ $\mathbf{T} = (T_1, \dots, T_{|\mathcal{P}|})^T \in \mathbb{R}^{|\mathcal{P}|}$
- ▶ $\mathbf{N} = (N_{c1}, \dots, N_{c|\mathcal{P}|})^T \in \mathbb{R}^{|\mathcal{P}|}$
- ▶ $\mathbf{d} = \text{diag}(d_1, \dots, d_{|\mathcal{P}|}) \in \mathbb{R}^{|\mathcal{P}| \times |\mathcal{P}|}$
- ▶ $\mathcal{M}_c \in \mathbb{R}^{|\mathcal{P}| \times |\mathcal{P}|}$

The nice case

Suppose movement rates **equal for all compartments**, i.e.,

$$\mathcal{M}_c \equiv \mathcal{M}$$

Then

$$\begin{aligned}\mathbf{T}' &= \mathbf{b} - \mathbf{dT} + \mathcal{M} \sum_{c \in \mathcal{C}} \mathbf{N}_c \\ &= \mathbf{b} - \mathbf{dT} + \mathcal{M} \mathbf{T}\end{aligned}\tag{11}$$

Equilibria

$$\begin{aligned}\mathbf{T}' = \mathbf{0} &\Leftrightarrow \mathbf{b} - \mathbf{dT} + \mathcal{M}\mathbf{T} = \mathbf{0} \\ &\Leftrightarrow (\mathbf{d} - \mathcal{M})\mathbf{T} = \mathbf{b} \\ &\Leftrightarrow \mathbf{T}^* = (\mathbf{d} - \mathcal{M})^{-1}\mathbf{b}\end{aligned}$$

given, of course, that $\mathbf{d} - \mathcal{M}$ (or, equivalently, $\mathcal{M} - \mathbf{d}$) is invertible..

Is it?

Nonsingularity of $\mathcal{M} - \mathbf{d}$

Using the spectrum shift of Theorem 6(1)

$$s\left(\mathcal{M} - \min_{p \in \mathcal{P}} d_p\right) = -\min_{p \in \mathcal{P}} d_p$$

This gives a constraint: for total population to behave well (in general, we want this), we *must assume all death rates are positive*

Assume they are (in other words, assume \mathbf{d} nonsingular). Then $\mathcal{M} - \mathbf{d}$ is nonsingular and $\mathbf{T}^* = (\mathbf{d} - \mathcal{M})^{-1}\mathbf{b}$ unique

Behaviour of the total population

Equal irreducible movement case

$\mathbf{T}^* = (\mathbf{d} - \mathcal{M})^{-1}\mathbf{b}$ attracts solutions of

$$\mathbf{T}' = \mathbf{b} - \mathbf{d}\mathbf{T} + \mathcal{M}\mathbf{T} =: f(\mathbf{T})$$

Indeed, we have

$$Df = \mathcal{M} - \mathbf{d}$$

Since we now assume that \mathbf{d} is nonsingular, we have by Theorem 6(1) that $s(\mathcal{M} - \min_{p \in \mathcal{P}} d_p) = -\min_{p \in \mathcal{P}} d_p < 0$

\mathcal{M} irreducible $\rightarrow \mathbf{T}^* \gg 0$ (provided $\mathbf{b} > \mathbf{0}$, of course)

Why it is important to incorporate space

Metapopulation models

Metapopulations à la Levins

Metapopulations à la Levin

The graph setting

Generic model

The movement matrix

Behaviour of the mobility component

A few sample models

Existence of a DFE

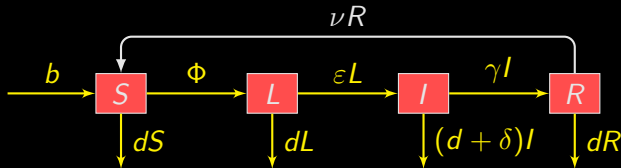
Computation of a reproduction number

Computational considerations

A few foot-and-mouth disease models

A few avian influenza models

The toy SLIRS model in patches



$$S' = b + \nu R - \Phi - dS \quad (12a)$$

$$L' = \Phi - (\varepsilon + d)L \quad (12b)$$

$$I' = \varepsilon L - (\gamma + d + \delta)I \quad (12c)$$

$$R' = \gamma I - (\nu + d)R \quad (12d)$$

Φ force of infection. Depends on S, I , possibly N . In general

$$\Phi = \beta(N)\phi(S, I)$$

Mass action, $\Phi = \beta SI$, proportional incidence, $\Phi = \beta SI/N$

$|\mathcal{P}|$ -SLIRS model

$$S'_p = b_p + \nu_p R_p - \Phi_p - d_p S_p + \sum_{q \in \mathcal{P}} m_{Spq} S_q \quad (13a)$$

$$L'_p = \Phi_p - (\varepsilon_p + d_p) L_p + \sum_{q \in \mathcal{P}} m_{Lpq} L_q \quad (13b)$$

$$I'_p = \varepsilon_p L_p - (\gamma_p + d_p) I_p + \sum_{q \in \mathcal{P}} m_{Ipq} I_q \quad (13c)$$

$$R'_p = \gamma_p I_p - (\nu_p + d_p) R_p + \sum_{q \in \mathcal{P}} m_{Rpq} R_q \quad (13d)$$

with incidence

$$\Phi_p = \beta_p \frac{S_p I_p}{N_p^{q_p}}, \quad q_p \in \{0, 1\} \quad (13e)$$

$|\mathcal{S}| |\mathcal{P}|$ -SLIRS (multiple species)

$p \in \mathcal{P}$ and $s \in \mathcal{S}$ (a set of species)

$$S'_{sp} = b_{sp} + \nu_{sp}R_{sp} - \Phi_{sp} - d_{sp}S_{sp} + \sum_{q \in \mathcal{P}} m_{Sspq}S_{sq} \quad (14a)$$

$$L'_{sp} = \Phi_{sp} - (\varepsilon_{sp} + d_{sp})L_{sp} + \sum_{q \in \mathcal{P}} m_{Lspq}L_{sq} \quad (14b)$$

$$I'_{sp} = \varepsilon_{sp}L_{sp} - (\gamma_{sp} + d_{sp})I_{sp} + \sum_{q \in \mathcal{P}} m_{Isdq}I_{sq} \quad (14c)$$

$$R_{sp} = \gamma_{sp}I_{sp} - (\nu_{sp} + d_{sp})R_{sp} + \sum_{q \in \mathcal{P}} m_{Rspq}R_{sq} \quad (14d)$$

with incidence

$$\Phi_{sp} = \sum_{k \in \mathcal{S}} \beta_{skp} \frac{S_{sp} I_{kp}}{N_p^{q_p}}, \quad q_p \in \{0, 1\} \quad (14e)$$

- ▶ JA, Davis, Hartley, Jordan, Miller & PvdD. A multi-species epidemic model with spatial dynamics. *Mathematical Medicine and Biology* 22(2):129-142 (2005)
- ▶ JA, Jordan & PvdD. Quarantine in a multi-species epidemic model with spatial dynamics. *Mathematical Biosciences* 206(1):46-60 (2007)

$|\mathcal{P}|^2$ -SLIRS (residents-travellers)

$$S'_{pq} = b_{pq} + \nu_{pq} R_{pq} - \Phi_{pq} - d_{pq} S_{pq} + \sum_{k \in \mathcal{P}} m_{Spqk} S_{pk} \quad (15a)$$

$$I'_{pq} = \Phi_{pq} - (\varepsilon_{pq} + d_{pq}) I_{pq} + \sum_{k \in \mathcal{P}} m_{Lpqk} L_{pk} \quad (15b)$$

$$L'_{pq} = \varepsilon_{pq} L_{pq} - (\gamma_{pq} + d_{pq}) I_{pq} + \sum_{k \in \mathcal{P}} m_{Ipqk} I_{pk} \quad (15c)$$

$$R'_{pq} = \gamma_{pq} I_{pq} - (\nu_{pq} + d_{pq}) R_{pq} + \sum_{k \in \mathcal{P}} m_{Rpqk} R_{pk} \quad (15d)$$

with incidence

$$\Phi_{pq} = \sum_{k \in \mathcal{P}} \beta_{pqk} \frac{S_{pq} I_{kq}}{N_p^{q_q}}, \quad q_q = \{0, 1\} \quad (15e)$$

- ▶ Sattenspiel & Dietz. A structured epidemic model incorporating geographic mobility among regions (1995)
- ▶ JA & PvdD. A multi-city epidemic model. *Mathematical Population Studies* 10(3):175-193 (2003)
- ▶ JA & PvdD. The basic reproduction number in a multi-city compartmental epidemic model. In *Positive Systems* (2003)

Steps for an analysis

Basic steps

1. Well-posedness of the system
2. Existence of disease free equilibria (DFE)
3. Computation of a reproduction number \mathcal{R}_0 , study local asymptotic stability of DFE
4. If DFE unique, prove global asymptotic stability when $\mathcal{R}_0 < 1$

Additional steps

5. Existence of *mixed* equilibria, with some locations at DFE and others with disease
6. Computation of some bounds on \mathcal{R}_0
7. EEP and its LAS & GAS properties

...

Analysis – Toy system

$$S'_p = b_p - \Phi_p - d_p S_p + \nu_p R_p + \sum_{q \in \mathcal{P}} m_{Spq} S_q \quad (16a)$$

$$L'_p = \Phi_p - (\varepsilon_p + d_p) L_p + \sum_{q \in \mathcal{P}} m_{Lpq} L_q \quad (16b)$$

$$I'_p = \varepsilon_p L_p - (\gamma_p + d_p) I_p + \sum_{q \in \mathcal{P}} m_{Ipq} I_q \quad (16c)$$

$$R'_p = \gamma_p I_p - (\nu_p + d_p) R_p + \sum_{q \in \mathcal{P}} m_{Rpq} R_q \quad (16d)$$

with incidence

$$\Phi_p = \beta_p \frac{S_p I_p}{N_p^{q_p}}, \quad q_p \in \{0, 1\} \quad (16e)$$

System of $4|\mathcal{P}|$ equations

Don't panic: size is not that bad..

System of $4|\mathcal{P}|$ equations !!!

However, a lot of structure:

- ▶ $|\mathcal{P}|$ copies of individual units, each comprising 4 equations
- ▶ Dynamics of individual units well understood
- ▶ Coupling is linear

⇒ Good case of large-scale system

(matrix analysis is your friend)

Existence and uniqueness

- ▶ Existence and uniqueness of solutions classic, assured by good choice of birth and force of infection functions
- ▶ In the cases treated later, the birth function is either constant or a linear combination of state variables
- ▶ May exist problems at the origin, if the force of infection is not defined there
- ▶ Assumption from now on: existence and uniqueness

Why it is important to incorporate space

Metapopulation models

Metapopulations à la Levins

Metapopulations à la Levin

The graph setting

Generic model

The movement matrix

Behaviour of the mobility component

A few sample models

Existence of a DFE

Computation of a reproduction number

Computational considerations

A few foot-and-mouth disease models

A few avian influenza models

Disease free equilibrium

The model is at equilibrium if the time derivatives are zero

Definition 8 (Metapopulation DFE)

In the case of system (16), location $p \in \mathcal{P}$ is at a disease-free equilibrium (DFE) if $L_p = I_p = 0$, and the $|\mathcal{P}|$ -location model is at a **metapopulation DFE** if $L_p = I_p = 0$ for all $p \in \mathcal{P}$

Here, we want to find the DFE for the $|\mathcal{P}|$ -location model. Later, the existence of mixed equilibria, with some locations at the DFE and others at an endemic equilibrium, is considered

(For (14), replace L_p with L_{sp} and I_p with I_{sp} , for (15), replace L_p by L_{pp} and I_p by I_{pp} . To simplify notation, we could write L_\bullet and I_\bullet)

Assume (16) at metapopulation DFE. Then $\Phi_p = 0$ and

$$0 = b_p - d_p S_p + \nu_p R_p + \sum_{q \in \mathcal{P}} m_{Spq} S_q$$

$$0 = -(\nu_p + d_p) R_p + \sum_{q \in \mathcal{P}} m_{Rpq} R_q$$

Want to solve for S_p, R_p . Here, it is best (crucial in fact) to remember some linear algebra. Write system in vector form:

$$\mathbf{0} = \mathbf{b} - \mathbf{d}\mathbf{S} + \nu\mathbf{R} + \mathcal{M}^S\mathbf{S}$$

$$\mathbf{0} = -(\nu + \mathbf{d})\mathbf{R} + \mathcal{M}^R\mathbf{R}$$

where $\mathbf{S}, \mathbf{R}, \mathbf{b} \in \mathbb{R}^{|\mathcal{P}|}$, $\mathbf{d}, \nu, \mathcal{M}^S, \mathcal{M}^R$ $|\mathcal{P}| \times |\mathcal{P}|$ -matrices (\mathbf{d}, ν diagonal)

R at DFE

Recall second equation:

$$\mathbf{0} = -(\nu + \mathbf{d})\mathbf{R} + \mathcal{M}^R\mathbf{R} \Leftrightarrow (\mathcal{M}^R - \nu - \mathbf{d})\mathbf{R} = \mathbf{0}$$

So unique solution $\mathbf{R} = \mathbf{0}$ if $\mathcal{M}^R - \nu - \mathbf{d}$ invertible Is it?

We have been here before!

From spectrum shift, $s(\mathcal{M}^R - \nu - \mathbf{d}) = -\min_{p \in \mathcal{P}}(\nu_p + d_p) < 0$

So, given $\mathbf{L} = \mathbf{I} = \mathbf{0}$, $\mathbf{R} = \mathbf{0}$ is the unique equilibrium and

$$\lim_{t \rightarrow \infty} \mathbf{R}(t) = \mathbf{0}$$

\implies DFE has $\mathbf{L} = \mathbf{I} = \mathbf{R} = \mathbf{0}$

S at the DFE

DFE has $\mathbf{L} = \mathbf{I} = \mathbf{R} = \mathbf{0}$ and $\mathbf{b} - \mathbf{d}\mathbf{S} + \mathcal{M}^S\mathbf{S} = \mathbf{0}$, i.e.,

$$\mathbf{S} = (\mathbf{d} - \mathcal{M}^S)^{-1}\mathbf{b}$$

Recall: $-\mathcal{M}^S$ singular M-matrix. From previous reasoning,
 $\mathbf{d} - \mathcal{M}^S$ has **instability modulus** shifted *right* by $\min_{p \in \mathcal{P}} d_p$. So:

- ▶ $\mathbf{d} - \mathcal{M}^S$ invertible
- ▶ $\mathbf{d} - \mathcal{M}^S$ nonsingular M-matrix

Second point $\implies (\mathbf{d} - \mathcal{M}^S)^{-1} > \mathbf{0} \implies (\mathbf{d} - \mathcal{M}^S)^{-1}\mathbf{b} > \mathbf{0}$
(would have $\gg \mathbf{0}$ if \mathcal{M}^S irreducible)

So DFE makes sense with

$$(\mathbf{S}, \mathbf{L}, \mathbf{I}, \mathbf{R}) = \left((\mathbf{d} - \mathcal{M}^S)^{-1}\mathbf{b}, \mathbf{0}, \mathbf{0}, \mathbf{0} \right)$$

Why it is important to incorporate space

Metapopulation models

Metapopulations à la Levins

Metapopulations à la Levin

The graph setting

Generic model

The movement matrix

Behaviour of the mobility component

A few sample models

Existence of a DFE

Computation of a reproduction number

Computational considerations

A few foot-and-mouth disease models

A few avian influenza models

Computing the basic reproduction number \mathcal{R}_0

Use next generation method with $\Xi = \{L_1, \dots, L_{|\mathcal{P}|}, I_1, \dots, I_{|\mathcal{P}|}\}$,
 $\Xi' = \mathcal{F} - \mathcal{V}$

$$\mathcal{F} = (\Phi_1, \dots, \Phi_{|\mathcal{P}|}, 0, \dots, 0)^T$$
$$\mathcal{V} = \begin{pmatrix} (\varepsilon_1 + d_1) L_1 - \sum_{q \in \mathcal{P}} m_{L1q} L_q \\ \vdots \\ (\varepsilon_{|\mathcal{P}|} + d_{|\mathcal{P}|}) L_{|\mathcal{P}|} - \sum_{q \in \mathcal{P}} m_{L|\mathcal{P}|q} L_q \\ -\varepsilon_1 L_1 + (\gamma_1 + d_1) I_1 - \sum_{q \in \mathcal{P}} m_{I1q} I_q \\ \vdots \\ -\varepsilon_{|\mathcal{P}|} L_{|\mathcal{P}|} + (\gamma_{|\mathcal{P}|} + d_{|\mathcal{P}|}) I_{|\mathcal{P}|} - \sum_{q \in \mathcal{P}} m_{I|\mathcal{P}|q} I_q \end{pmatrix}$$

Differentiate w.r.t. Ξ :

$$D\mathcal{F} = \begin{pmatrix} \frac{\partial \Phi_1}{\partial L_1} & \dots & \frac{\partial \Phi_1}{\partial L_{|\mathcal{P}|}} & \frac{\partial \Phi_1}{\partial l_1} & \dots & \frac{\partial \Phi_1}{\partial l_{|\mathcal{P}|}} \\ \vdots & & \vdots & \vdots & & \vdots \\ \frac{\partial \Phi_{|\mathcal{P}|}}{\partial L_1} & \dots & \frac{\partial \Phi_{|\mathcal{P}|}}{\partial L_{|\mathcal{P}|}} & \frac{\partial \Phi_{|\mathcal{P}|}}{\partial l_1} & \dots & \frac{\partial \Phi_{|\mathcal{P}|}}{\partial l_{|\mathcal{P}|}} \\ 0 & \dots & 0 & 0 & \dots & 0 \\ \vdots & & \vdots & \vdots & & \vdots \\ 0 & \dots & 0 & 0 & \dots & 0 \end{pmatrix}$$

Note that

$$\frac{\partial \Phi_p}{\partial L_k} = \frac{\partial \Phi_p}{\partial I_k} = 0$$

whenever $k \neq p$, so

$$D\mathcal{F} = \begin{pmatrix} \text{diag} \left(\frac{\partial \Phi_1}{\partial L_1}, \dots, \frac{\partial \Phi_{|\mathcal{P}|}}{\partial L_{|\mathcal{P}|}} \right) & \text{diag} \left(\frac{\partial \Phi_1}{\partial I_1}, \dots, \frac{\partial \Phi_{|\mathcal{P}|}}{\partial I_{|\mathcal{P}|}} \right) \\ \mathbf{0} & \mathbf{0} \end{pmatrix}$$

Evaluate $D\mathcal{F}$ at DFE

If $\Phi_p = \beta_p S_p I_p$, then

- ▶ $\frac{\partial \Phi_p}{\partial L_p} = 0$
- ▶ $\frac{\partial \Phi_p}{\partial I_p} = \beta_p S_p$

If $\Phi_p = \beta_p \frac{S_p I_p}{N_p}$, then

- ▶ $\frac{\partial \Phi_p}{\partial L_p} = \beta_p \frac{S_p I_p}{N_p^2} = 0$ at DFE
- ▶ $\frac{\partial \Phi_p}{\partial I_p} = \beta_p \frac{S_p}{N_p}$ at DFE

In both cases, $\partial/\partial L$ block is zero so

$$F = D\mathcal{F}(DFE) = \begin{pmatrix} \mathbf{0} & \text{diag} \left(\frac{\partial \Phi_1}{\partial I_1}, \dots, \frac{\partial \Phi_{|\mathcal{P}|}}{\partial I_{|\mathcal{P}|}} \right) \\ \mathbf{0} & \mathbf{0} \end{pmatrix}$$

Compute $D\mathcal{V}$ and evaluate at DFE

$$V = \begin{pmatrix} \text{diag}_p(\varepsilon_p + d_p) - \mathcal{M}^L & \mathbf{0} \\ -\text{diag}_p(\varepsilon_p) & \text{diag}_p(\gamma_p + d_p) - \mathcal{M}^I \end{pmatrix}$$

where $\text{diag}_p(z_p) := \text{diag}(z_1, \dots, z_{|\mathcal{P}|})$

Inverse of V easy (2×2 block lower triangular):

$$V^{-1} = \begin{pmatrix} (\text{diag}_p(\varepsilon_p + d_p) - \mathcal{M}^L)^{-1} & \mathbf{0} \\ \tilde{V}_{21}^{-1} & (\text{diag}_p(\gamma_p + d_p) - \mathcal{M}^I)^{-1} \end{pmatrix}$$

where

$$\begin{aligned} \tilde{V}_{21}^{-1} = & \left(\text{diag}_p(\varepsilon_p + d_p) - \mathcal{M}^L \right)^{-1} \\ & \text{diag}_p(\varepsilon_p) \left(\text{diag}_p(\gamma_p + d_p) - \mathcal{M}^I \right)^{-1} \end{aligned}$$

$$\mathcal{R}_0 \text{ as } \rho(FV^{-1})$$

Next generation matrix

$$FV^{-1} = \begin{pmatrix} \mathbf{0} & F_{12} \\ \mathbf{0} & \mathbf{0} \end{pmatrix} \begin{pmatrix} \tilde{V}_{11}^{-1} & \mathbf{0} \\ \tilde{V}_{21}^{-1} & \tilde{V}_{22}^{-1} \end{pmatrix} = \begin{pmatrix} F_{12}\tilde{V}_{21}^{-1} & F_{12}\tilde{V}_{22}^{-1} \\ \mathbf{0} & \mathbf{0} \end{pmatrix}$$

where \tilde{V}_{ij}^{-1} is block ij in V^{-1} . So

$$\mathcal{R}_0 = \rho(F_{12}\tilde{V}_{21}^{-1})$$

i.e.,

$$\mathcal{R}_0 = \rho \left(\text{diag} \left(\frac{\partial \Phi_1}{\partial I_1}, \dots, \frac{\partial \Phi_{|\mathcal{P}|}}{\partial I_{|\mathcal{P}|}} \right) \left(\text{diag}_p(\varepsilon_p + d_p) - \mathcal{M}^L \right)^{-1} \right. \\ \left. \text{diag}_p(\varepsilon_p) \left(\text{diag}_p(\gamma_p + d_p) - \mathcal{M}' \right)^{-1} \right)$$

Local asymptotic stability of the DFE

Theorem 9

Define \mathcal{R}_0 for the $|\mathcal{P}|$ -SLIRS as

$$\mathcal{R}_0 = \rho \left(\text{diag} \left(\frac{\partial \Phi_1}{\partial I_1}, \dots, \frac{\partial \Phi_{|\mathcal{P}|}}{\partial I_{|\mathcal{P}|}} \right) \left(\text{diag}_p(\varepsilon_p + d_p) - \mathcal{M}^L \right)^{-1} \right. \\ \left. \text{diag}_p(\varepsilon_p) \left(\text{diag}_p(\gamma_p + d_p) - \mathcal{M}' \right)^{-1} \right)$$

Then the DFE

$$(\mathbf{S}, \mathbf{L}, \mathbf{I}, \mathbf{R}) = \left((\mathbf{d} - \mathcal{M}^S)^{-1} \mathbf{b}, \mathbf{0}, \mathbf{0}, \mathbf{0} \right)$$

is locally asymptotically stable if $\mathcal{R}_0 < 1$ and unstable if $\mathcal{R}_0 > 1$

Some remarks about \mathcal{R}_0

The expression for \mathcal{R}_0 in Theorem 9 is exact

However, unless you consider a very small set of locations, you will not get a closed form expression

Indeed, by Theorem 6(3) and more importantly (often \mathcal{M} is irreducible), Theorem 6(4), the two inverses in \mathcal{R}_0 are likely crowded ($\gg 0$ in the irreducible case)

However, numerically, this works easy unless conditioning is bad

The toy $|\mathcal{P}|$ -SLIRS

LAS results for $\mathcal{R}_0 < 1$ can sometimes be strengthened to GAS.
One class of models where this works often is when the population
is either constant or asymptotically constant and incidence is
standard

Theorem 10

Let \mathcal{R}_0 be defined as in Theorem 9 and use proportional incidence
 $\Phi_p = \beta_p S_p I_p / N_p$. If $\mathcal{R}_0 < 1$, then the DFE of system (16) is
globally asymptotically stable

$|\mathcal{S}| |\mathcal{P}|$ -SLIRS with multiple species

In the case in which movement is equal for all compartments and there is no disease death, a comparison theorem argument can be used as in Theorem 10 to show that if $\mathcal{R}_0 < 1$, then the DFE of the $|\mathcal{S}| |\mathcal{P}|$ -SLIRS (14) is globally asymptotically stable.

Theorem 11

For system (14) with $|\mathcal{S}|$ species and $|\mathcal{P}|$ locations, with movement equal for all compartments, define \mathcal{R}_0 appropriately and use proportional incidence. If $\mathcal{R}_0 < 1$, then the DFE is globally asymptotically stable

Why it is important to incorporate space

Metapopulation models

Metapopulations à la Levins

Metapopulations à la Levin

The graph setting

Generic model

The movement matrix

Behaviour of the mobility component

A few sample models

Existence of a DFE

Computation of a reproduction number

Computational considerations

A few foot-and-mouth disease models

A few avian influenza models

Set up parameters

```
pop = c(34.017, 1348.932, 1224.614, 173.593, 93.261) * 1e+06
countries = c("Canada", "China", "India", "Pakistan", "
    Philippines")
T = matrix(data =
    c(0, 1268, 900, 489, 200,
      1274, 0, 678, 859, 150,
      985, 703, 0, 148, 58,
      515, 893, 144, 0, 9,
      209, 174, 90, 2, 0),
    nrow = 5, ncol = 5, byrow = TRUE)
```

Work out movement matrix

```
p = list()
# Use the approximation explained in Arino & Portet (JMB 2015)
p$M = mat.or.vec(nr = dim(T)[1], nc = dim(T)[2])
for (from in 1:5) {
  for (to in 1:5) {
    p$M[to, from] = -log(1 - T[from, to]/pop[from])
  }
  p$M[from, from] = 0
}
p$M = p$M - diag(colSums(p$M))
```

```
p$P = dim(p$M)[1]
p$eta = rep(0.3, p$P)
p$epsilon = rep((1/1.5), p$P)
p$pi = rep(0.7, p$P)
p$gammaI = rep((1/5), p$P)
p$gammaA = rep((1/3), p$P)
# The desired values for R_0
R_0 = rep(1.5, p$P)
```

Write down indices of the different state variable types

Save index of state variable types in state variables vector (we have to use a vector and thus, for instance, the name "S" needs to be defined)

```
p$idx_S = 1:p$P  
p$idx_L = (p$P+1):(2*p$P)  
p$idx_I = (2*p$P+1):(3*p$P)  
p$idx_A = (3*p$P+1):(4*p$P)  
p$idx_R = (4*p$P+1):(5*p$P)
```

Set up IC and time

```
# Set initial conditions. For example, we start with 2
# infectious individuals in Canada.

L0 = mat.or.vec(p$P, 1)
I0 = mat.or.vec(p$P, 1)
A0 = mat.or.vec(p$P, 1)
R0 = mat.or.vec(p$P, 1)
I0[1] = 2
S0 = pop - (L0 + I0 + A0 + R0)
# Vector of initial conditions to be passed to ODE solver.
IC = c(S = S0, L = L0, I = I0, A = A0, R = R0)
# Time span of the simulation (5 years here)
tspan = seq(from = 0, to = 5 * 365.25, by = 0.1)
```

Set up β to avoid blow up

Let us take $\mathcal{R}_0 = 1.5$ for patches in isolation. Solve \mathcal{R}_0 for β

$$\beta = \frac{\mathcal{R}_0}{S(0)} \left(\frac{1 - \pi_p}{\gamma_{lp}} + \frac{\pi_p \eta_p}{\gamma_{Ap}} \right)^{-1}$$

```
for (i in 1:p$P) {  
  p$beta[i] =  
    R_0[i] / S0[i] * 1/((1 - p$pi[i])/p$gammaI[i] + p$pi[i] *  
    p$eta[i]/p$gammaA[i])  
}
```

Define the vector field

```
SLIAR_metapop_rhs <- function(t, x, p) {
  with(as.list(p), {
    S = x[idx_S]
    L = x[idx_L]
    I = x[idx_I]
    A = x[idx_A]
    R = x[idx_R]
    N = S + L + I + A + R
    Phi = beta * S * (I + eta * A) / N
    dS = -Phi + MS %*% S
    dL = Phi - epsilon * L + p$ML %*% L
    dI = (1 - pi) * epsilon * L - gammaI * I + MI %*% I
    dA = pi * epsilon * L - gammaA * A + MA %*% A
    dR = gammaI * I + gammaA * A + MR %*% R
    dx = list(c(dS, dL, dI, dA, dR))
    return(dx)
  })
}
```

And now call the solver

```
# Call the ODE solver
sol <- ode(y = IC,
            times = tspan,
            func = SLIAR_metapop_rhs,
            parms = p,
            method = "ode45")
```

One little trick (case with demography)

Suppose demographic EP is $\mathbf{N}^* = (\mathbf{d} - \mathcal{M})^{-1}\mathbf{b}$

Want to maintain $\mathbf{N}(t) = \mathbf{N}^*$ for all t to ignore convergence to demographic EP. Think in terms of \mathbf{b} :

$$\mathbf{N}' = 0 \iff \mathbf{b} - \mathbf{d}\mathbf{N} + \mathcal{M}\mathbf{N} = 0 \iff \mathbf{b} = (\mathbf{d} - \mathcal{M})\mathbf{N}$$

So take $\mathbf{b} = (\mathbf{d} - \mathcal{M})\mathbf{N}^*$

Then

$$\mathbf{N}' = (\mathbf{d} - \mathcal{M})\mathbf{N}^* - \mathbf{d}\mathbf{N} + \mathcal{M}\mathbf{N}$$

and thus if $\mathbf{N}(0) = \mathbf{N}^*$, then $\mathbf{N}'(0) = 0$ and thus $\mathbf{N}' = 0$ for all $t \geq 0$, i.e., $\mathbf{N}(t) = \mathbf{N}^*$ for all $t \geq 0$

Word of warning about that trick, though..

$$\mathbf{b} = (\mathbf{d} - \mathcal{M})\mathbf{N}^*$$

$\mathbf{d} - \mathcal{M}$ has nonnegative (typically positive) diagonal entries and nonpositive off-diagonal entries

Easy to think of situations where the diagonal will be dominated by the off-diagonal, so \mathbf{b} could have negative entries

⇒ use this for numerics, not for the mathematical analysis

Why it is important to incorporate space

Metapopulation models

A few foot-and-mouth disease models

Woolhouse and collaborators

Ringa & Bauch

Cabezas *et al*

Bradhurst *et al*

Buhnerkempe *et al*

Glass & Barnes

A few avian influenza models

Most models are à la Levins

Space is implicit: count infected herds

In simplest models, space is entirely implicit

Herds are spatially located, so there is space

An analysis of foot-and-mouth-disease epidemics in the UK

D. T. HAYDON† AND M. E. J. WOOLHOUSE

Department of Zoology, University of Oxford, South Parks Road, Oxford OX1 3PS, UK

R. P. KITCHING

Institute for Animal Health, Pirbright Laboratory, Pirbright, Surrey GU24 0NF, UK

The model

$$\Delta S(t) = -\beta(t)S(t)I(t) \quad (17a)$$

$$\Delta L(t) = \beta(t)S(t)I(t) - \beta(t-\sigma)S(t-\sigma)I(t-\sigma) \quad (17b)$$

$$\begin{aligned} \Delta I(t) = & \beta(t-\sigma)S(t-\sigma)I(t-\sigma) \\ & - \beta(t-\sigma-\nu)S(t-\sigma-\nu)I(t-\sigma-\nu) \end{aligned} \quad (17c)$$

$$\Delta R(t) = \beta(t-\sigma-\nu)S(t-\sigma-\nu)I(t-\sigma-\nu) \quad (17d)$$

where $\Delta X(t) = X(t+1) - X(t)$, σ is the fixed latent period and ν is the fixed infectious period

Reproduction number

Provided $N \gg 1$,

$$\mathcal{R}_0 = \frac{\beta(0)N}{\nu}$$

Estimates of $\beta(t)$ obtained using

$$\beta(t) = \frac{\Delta L(t) + \beta(t - \sigma)S(t - \sigma)I(t - \sigma)}{S(t)I(t)}$$

Used for the 1967-1968 UK epidemic, time unit of 1 day, $\sigma = 5$ days, $\nu = 4$ days and $N = 16,507$ herds

Here, space is purely implicit, in the sense that the only source of spatiality is the fact that the data comes from farms that are spatially located

From: Foot-and-Mouth Disease: Current Perspectives. Edited by: Francisco Sobrino and Esteban Domingo

Chapter 13

Mathematical Models of the Epidemiology and Control of Foot-and-Mouth Disease

Mark E. J. Woolhouse

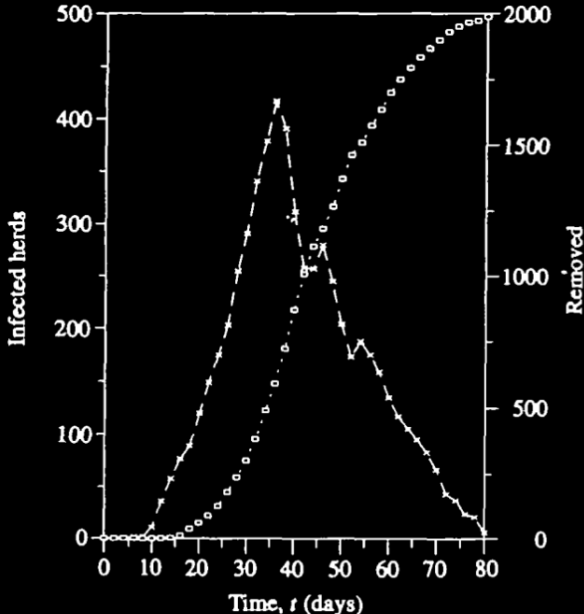


FIG. 1. (—□—) Cumulative numbers of the herds removed, $R(t)$, and (×) the reconstructed number of infectives calculated from equation (3) during the 1967-68 UK (FMD) epidemic.

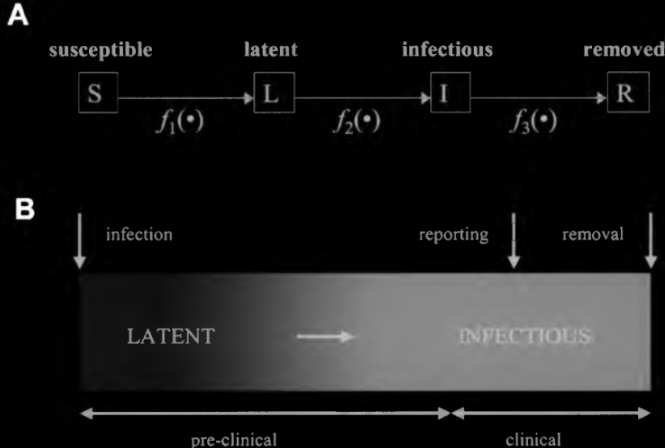


Figure 1. Compartments, in theory and practice. A) A diagrammatic representation of a simple SLIR model showing the flow of hosts between susceptible, latent infected, infectious and removed compartments. The numbers (or fractions or densities) of hosts in these compartments are represented by the variables S , L , I and R respectively. The rate of flow is specified by three expressions: $f_1(\bullet)$, the rate at which susceptible hosts become infected; $f_2(\bullet)$, the rate at which latently infected hosts become infectious; and $f_3(\bullet)$, the rate at which infectious hosts are removed. Different models use different mathematical expressions, representing different levels of detail and incorporating different numbers of parameters. B) A diagrammatic representation of the course of a FMD infection in a single host (or single farm). Note that the transition between latent and infectious does not correspond to the appearance of clinical signs: animals may be infectious before clinical signs appear. In practice, there is inevitably a further delay before clinical signs are observed and reported.

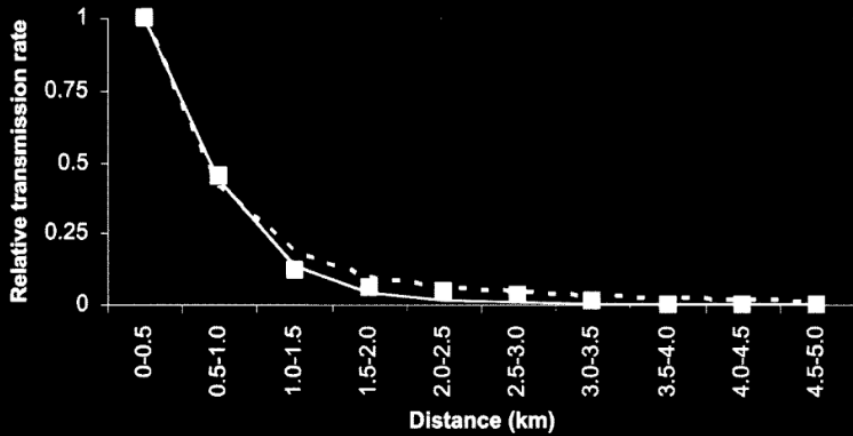


Figure 3. Examples of transmission kernels, relative per capita rate of transmission as a function of distance between farms. Empirical results (symbols) derived using data tracing studies carried out during the UK 2001 epidemic after the imposition of a national ban on livestock movements (Keeling *et al.*, 2001) are compared with two standard functions: 1) k/d^2 with $k=0.41$ (broken line); and 2) $g\exp[-hd]$ with $g=4.8$ and $h=2.4$ (solid line). All functions show per capita transmission rates relative to that over distances of 0 to 0.5km. The constants k , g and h were fitted using the least squares method. The empirically-derived transmission kernel equates to 70% of transmission occurring over distances up to 3km. Note that function (1) overestimates transmission rates at longer distances, whereas function (2) underestimates these.

Dynamics of the 2001 UK Foot and Mouth Epidemic: Stochastic Dispersal in a Heterogeneous Landscape

Matt J. Keeling,^{1*} Mark E. J. Woolhouse,² Darren J. Shaw,²
Louise Matthews,² Margo Chase-Topping,² Dan T. Haydon,³
Stephen J. Cornell,¹ Jens Kappey,¹ John Wilesmith,⁴
Bryan T. Grenfell¹

Foot-and-mouth is one of the world's most economically important livestock diseases. We developed an individual farm-based stochastic model of the current UK epidemic. The fine grain of the epidemiological data reveals the infection dynamics at an unusually high spatiotemporal resolution. We show that the spatial distribution, size, and species composition of farms all influence the observed pattern and regional variability of outbreaks. The other key dynamical component is long-tailed stochastic dispersal of infection, combining frequent local movements with occasional long jumps. We assess the history and possible duration of the epidemic, the performance of control strategies, and general implications for disease dynamics in space and time.

Incorporating space

Transmission between farms determined by number and type of livestock and distance between susceptible and infectious farms

Probability that a susceptible farm i becomes infected a given day

$$\mathbb{P} = 1 - \exp \left(-SN_i \sum_{j \in \text{infectious}} TN_j K(d_{ij}) \right) \quad (18)$$

K infection kernel, d_{ij} distance between farms i and j

Table 1. Results from the stochastic spatial model (2, 10) considering a variety of control options. The total reported cases (on an individual farm basis) for each control policy and the total cull (including IP slaughtering, DC, and CP culls) are given as a percentage of the results from the full model using the observed control policy, including the extended 3-km and welfare culls. The total number of farms vaccinated is given as a percentage of the total cull in the full model. All of the control policies tested below ignore the extended 3-km and welfare culls used in some locations. The standard control policy follows the timing and level of the observed measure. The prompt cull follows the level of the observed measures but achieves a 24/48-hour delay from reporting to slaughter/cull throughout the epidemic. The intensive cull follows the timing of the observed measures but matches the levels achieved in the latter stages of the epidemic. The 3-km ring cull removes infected premises and all other farms within a 3-km radius. The next three measures include vaccination of cattle (at 90% coverage) within a 3-km ring around all infected premises in addition to the slaughter and cull policy. Vaccination of all species gives somewhat better, but qualitatively similar, results. Finally, we consider barrier vaccination (as in Fig. 3D) at 90% coverage. More details about the various control measures are given in the supplementary material (10).

Control measure	Total cases	Total cull	Total vaccinated
Standard	105%	84%	0%
IP cull only	927%	342%	0%
Prompt cull (24/48-hour delay throughout)	57%	54%	0%
Intensive cull (high levels throughout)	45%	73%	0%
3-km ring cull only	47%	142%	0%
Standard + 90% vaccination	84%	72%	76%
Standard + vaccination from May	97%	81%	8%
IP only + vaccination	784%	156%	453%
Standard + barrier vaccination	70%	69%	251%

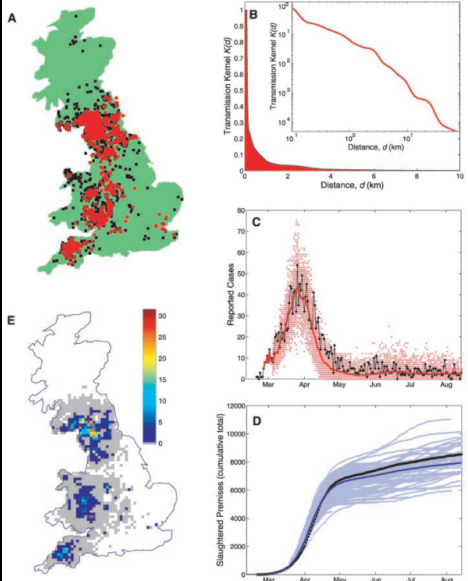
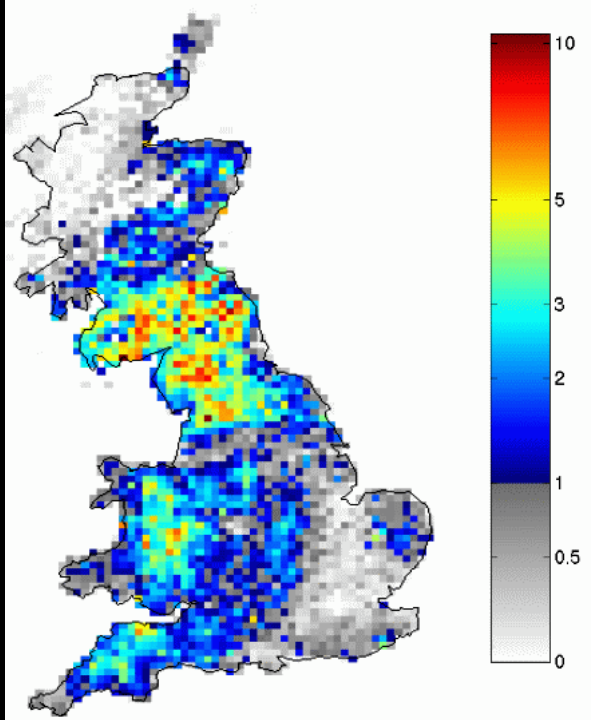


Fig. 1. A comparison between the observed epidemic and 100 replicates of the stochastic model. Simulations start on 23 February 2001 (when movement restrictions were fully in place) and use the reported cases to that date and the position of all susceptible farms as initial conditions. **(A)** The actual spatial distribution of IPs (red) and culled premises (black). **(B)** The transmission kernel K as a function of distance (d), calculated from the distance between sources of infectious and their secondary cases. **(C)** Comparison of the number of infected premises. **(D)** Comparison of the cumulative total of culled or slaughtered premises. Black dots show the actual number, pale dots (red or blue) show the results from simulations, and solid lines (red or blue) show the average of the simulations. **(E)** The average number of simulated cases in 10-km-by-10-km squares. The model results shown are from 100 simulations.



Received 7 February 2003

Accepted 14 April 2003

Published online 7 July 2003

Neighbourhood control policies and the spread of infectious diseases

L. Matthews^{1*}, D. T. Haydon², D. J. Shaw¹, M. E. Chase-Topping¹,
M. J. Keeling^{3,4} and M. E. J. Woolhouse¹

¹Centre for Tropical Veterinary Medicine, University of Edinburgh, Easter Bush, Roslin EH25 9RG, UK

²Department of Zoology, University of Guelph, Guelph, Ontario N1G 2W1, Canada

³Mathematics Institute, and ⁴Department of Biological Sciences, University of Warwick, Gibbet Hill, Coventry CV4 7AL, UK

Another model

$$S' = -\beta(1 - f(c)) \frac{SI}{N} - c \frac{SI}{N} \quad (19a)$$

$$I' = \beta(1 - f(c)) \frac{SI}{N} - \sigma I \quad (19b)$$

$$R' = \sigma I + c \frac{SI}{N} \quad (19c)$$

$f(c)$ proportion of exposed holdings removed, c the removal rate
(level of control)

$\mathcal{R}_0 = \beta/\sigma$ and

$$\mathcal{R}_c = \beta \frac{1 - f}{\sigma} = (1 - f)\mathcal{R}_0$$

Then consider a metapopulation version

Break down susceptible population into clusters of holdings within which short-range transmission occurs, and between which long-range transmission occurs

Transmission rate β broken down into a short-range transmission rate, β_s , corresponding to infections generated within the cluster, and a long-range transmission rate, β_l , corresponding to infections generated outside the cluster in question

Modelling vaccination strategies against foot-and-mouth disease

M. J. Keeling*, M. E. J. Woolhouse†, R. M. May‡, G. Davies§ & B. T. Grenfell||

* Department of Biological Science & Mathematics Institute, University of Warwick, Gibbet Hill Road, Coventry, CV4 7AL, UK

† Centre for Infectious Diseases, College of Medicine and Veterinary Medicine, University of Edinburgh, Easter Bush, Roslin, Midlothian, EH25 9RG, UK

‡ Department of Zoology, University of Oxford, Oxford, OX1 3PS, UK

§ Zinnia, Kettlewell Hill, Woking, Surrey, GU21 4JJ, UK

|| Department of Zoology, University of Cambridge, Downing Street, Cambridge, CB2 3EJ, UK

Vaccination has proved a powerful defence against a range of infectious diseases of humans and animals. However, its potential to control major epidemics of foot-and-mouth disease (FMD) in livestock is contentious. Using an individual farm-based model, we consider either national prophylactic vaccination campaigns in advance of an outbreak, or combinations of reactive vaccination and culling strategies during an epidemic. Consistent with standard epidemiological theory, mass prophylactic vaccination could reduce greatly the potential for a major epidemic, while the targeting of high-risk farms increases efficiency. Given sufficient resources and preparation, a combination of reactive vaccination and culling might control ongoing epidemics. We also explore a reactive strategy, 'predictive' vaccination, which targets key spatial transmission loci and can reduce markedly the long tail that characterizes many FMD epidemics. These analyses have broader implications for the control of human and livestock infectious diseases in heterogeneous spatial landscapes.

The basic model

The model used throughout this paper is a spatial stochastic simulation, where the infectious state of every livestock farm in Britain is predicted on a daily basis. The rate, r , at which farm i (which is currently susceptible) is infected is given by,

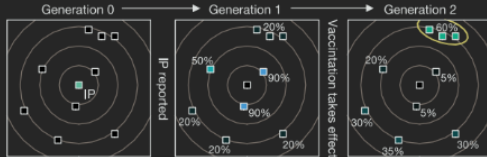
$$R_i = \sum_{L \in \text{livestock}} S_L N_L^i \times \sum_{j \in \text{infectious}} \sum_{L \in \text{livestock}} T_L N_L^j \times K(d_{ij})$$

where N_L^i is the number of livestock of type L within farm i ; S_L is the susceptibility of livestock L ; T_L is the transmission rate of livestock L ; d_{ij} is the distance between farms i and j ; and K is the transmission kernel. Once infected, farms are assumed to remain in an exposed (but not infectious) state for 4 days, after which they become infectious and can transmit the virus to other farms. Nine days after infection, after the appearance of clinical signs, the presence of the disease is reported; after a further delay of between 1 and 3 days (depending on the stage of the epidemic) the animals on the infected farm are slaughtered and the appropriate neighbourhood cull is performed (see Supplementary Information). It was estimated that around 40% of dangerous contacts were infected. More details of the parameter estimation and model validation can be found elsewhere⁷.

Predictive vaccination

Schematic diagrams showing the probability of being infected in each generation. In generation 0 the central farm is infected (it is an IP), whereas the surrounding farms are assumed susceptible. At the end of generation 1, the animals in the IP show signs and the farm reports infection—at this stage vaccination should occur. In generation 1, farms are infected in relation to their distance from the IP. The two farms that are closest have very high probabilities of already being infected, and therefore are unlikely to be infected in the next generation. It is the cluster of farms (circled blue) that have the greatest chance of being infected in generation 2 because: there is a 99% chance that at least one of them is still susceptible in generation 1; they can get infected in generation 2 from farms close to the original IP; and there is a 49% chance that at least one of them got infected in generation 1, subsequent spread to the remainder in generation 2 is then likely. Therefore, in response to the IP, the circled cluster of farms should be vaccinated with the highest priority as here the vaccine has the maximal effect—vaccinating the nearest farms would be futile as they will already be infected before the vaccine takes effect.

The efficacy of predictive vaccination depends on how reliably risk factors for infection and transmission can be identified. Here we have assumed complete knowledge of those risk factors (although the actual outcome is still stochastic in nature). The effectiveness of the strategy will be less if risk factors are less well known.



Why it is important to incorporate space

Metapopulation models

A few foot-and-mouth disease models

Woolhouse and collaborators

Ringa & Bauch

Cabezas *et al*

Bradhurst *et al*

Buhnerkempe *et al*

Glass & Barnes

A few avian influenza models



Contents lists available at ScienceDirect

Journal of Theoretical Biology

journal homepage: www.elsevier.com/locate/yjtbi



Dynamics and control of foot-and-mouth disease in endemic countries: A pair approximation model



N. Ringa ^{a,*}, C.T. Bauch ^{a,b}

^a Department of Mathematics and Statistics, University of Guelph, 50 Stone Rd E, Guelph, Canada N1G 2W1

^b Department of Applied Mathematics, University of Waterloo, 200 University Avenue West Waterloo, Canada N2L 3G1

HIGHLIGHTS

- Traditional models of FMD focus on control and dynamics in disease-free settings.
- We analyze long-term dynamics and control of FMD in endemic countries.
- Success of vaccination depends on rates of vaccine and natural immunity waning.
- Prophylactic vaccination performs better than ring vaccination.
- More mathematical models applicable to FMD-endemic countries need to be developed.

Pair approximation models

Suppose farms are in status X or Y (e.g., susceptible and infected). Pair approximation models consider the *expected number* $[XY]$ of pairs of the form X and Y at time t

A sample derivation (appendix in the paper)

The dynamics of $[SI]$ are governed by the equation

$$g'(t) = \sum r(\varepsilon) \Delta g(\varepsilon)$$

where $g(t)$ state variable of interest ($[SI]$ here), $r(\varepsilon)$ rate of event ε and $\Delta g(\varepsilon)$ change this event causes in $g(t)$

We're interested in transformation of edges, e.g., infection through an $S - I$ edge converts S into E , i.e. $SI \mapsto EI$ (\mapsto means "transformed to")

What affects $[SI]'$

- ▶ Infection of susceptible farm by infectious farm in the $S - I$ edge converts S into E , i.e. $SI \mapsto EI$. Adds $-\tau[SI]$, since this “destroys” $S - I$ edges
- ▶ Infection of susceptible farm “from the left” in a triple $I - S - I$, i.e. $I \leftrightarrow SI$ gives rise to $SI \mapsto EI$, i.e., $-\tau[ISI]$
- ▶ Latent period $1/\nu$, so $SE \mapsto SI$, “creating” an $S - I$
- ▶ Infectious farm recovers at rate σ , therefore $SI \mapsto SR$ contributes $\sigma[SI]$
- ▶ Ring vaccination (vaccination of E and S farms with links with I farms) in the S farm in a pair $S - I$, at rate ψ_r converts $S - I$ to $I - V$ and adds $\psi_r[SI]$
- ▶ Ring vaccination in the susceptible farm in a triple $I - S - I$, at rate ψ_r converts $S - I$ to $I - V$ and adds $\psi_r[ISI]$
- ▶ A recovered farm in an $I - R$ pair loses natural immunity at rate ω to form an $S - I$ pair, thus adding $\omega[IR]$
- ▶ A vaccinated farm in an $I - V$ pair loses vaccine protection at rate θ to form an $S - I$ pair, thus adding $\theta[IV]$

Therefore the equation of motion for $[SI]$ is

$$\begin{aligned}[SI]' = & -\tau([ISI] + [SI]) + \nu[SE] - \sigma[SI] - \psi_r([SI] + [ISI]) \\ & - \psi_p[SI] + \omega[IR] + \theta[IV]\end{aligned}$$

Why it is important to incorporate space

Metapopulation models

A few foot-and-mouth disease models

Woolhouse and collaborators

Ringa & Bauch

Cabezas et al

Bradhurst *et al*

Buhnerkempe *et al*

Glass & Barnes

A few avian influenza models

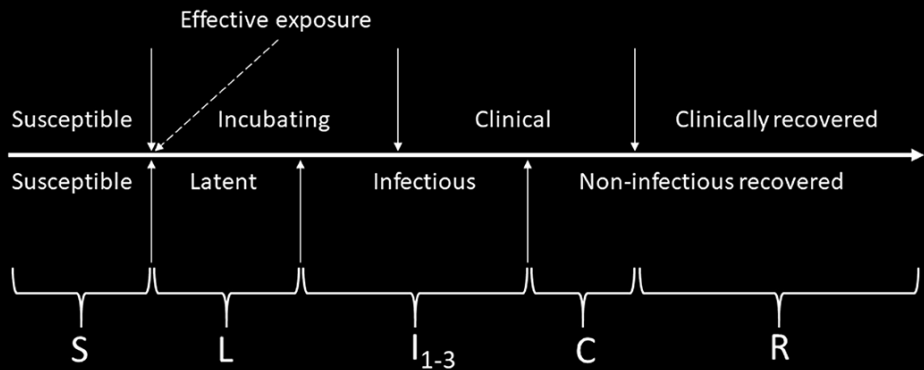


A Meta-Population Model of Potential Foot-and-Mouth Disease Transmission, Clinical Manifestation, and Detection Within U.S. Beef Feedlots

OPEN ACCESS

Aurelio H. Cabezas^{1,2}, Michael W. Sanderson^{1,2} and Victoriya V. Volkova^{1,2†}*

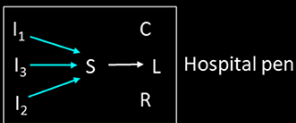
Disease progression



Infection progression

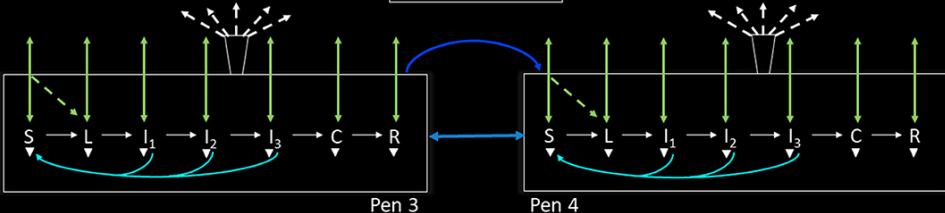
Pen 1

Pen 2



Pen 3

Pen 4



$$\begin{aligned}
\frac{dS}{dt} = & -\beta_{wp} S(I_1 + I_2 + I_3) - \varphi S - \text{Bin}\left(\varphi_{(t-1)} S_{(t-1)}, p_{\text{inf}} \text{hp}_{l_{(t-1)}}\right) - \\
& \left\{ \begin{array}{ll} S\beta_{bp}(I_1 + I_2 + I_3); & j \text{ present} \\ 0; & \text{otherwise} \end{array} \right\} - \left\{ \begin{array}{ll} S\beta_{bp}(I_1 + I_2 + I_3)_h; & h \text{ present} \\ 0; & \text{otherwise} \end{array} \right\} - \\
& \left\{ \begin{array}{ll} \text{Bin}(S, 0.5); & j \text{ present, shares water-trough with } i, \text{ and FMDv load in 1 L of the water } \geq ID_{50} \text{ per oral} \\ 0; & \text{otherwise} \end{array} \right\} - \\
& \left\{ \begin{array}{ll} \text{Bin}(S, 0.5); & h \text{ present, shares water-trough with } i, \text{ and FMDv load in 1 L of the water } \geq ID_{50} \text{ per oral} \\ 0; & \text{otherwise} \end{array} \right\} - \\
& \left\{ \begin{array}{ll} \text{Bin}\left[\left(\frac{\text{FMDv_floor}_j \times \sigma}{ID_{50} \text{ per oral}}\right), 0.5\right]; & j \text{ present and } \left(\frac{\text{FMDv_floor}_j \times \sigma}{ID_{50} \text{ per oral}}\right) \leq S \\ 0; & \text{otherwise} \end{array} \right\} - \\
& \left\{ \begin{array}{ll} \text{Bin}(S, p_{\text{air}_i}); & \sum_{k=1}^n I_3 \geq 0 \\ 0; & \text{otherwise} \end{array} \right\} - \mu S
\end{aligned}$$

Latent:

$$\frac{dL}{dt} = \beta_{wp} S(I_1 + I_2 + I_3) - \varphi L + \text{Bin}\left(\varphi_{(t-1)} S_{(t-1)}, p_{\text{inf}} h p_{I_{(t-1)}}\right) + \\ \left\{ \begin{array}{ll} S \beta_{bp} (I_1 + I_2 + I_3); & j \text{ present} \\ 0; & \text{otherwise} \end{array} \right\} + \left\{ \begin{array}{ll} S \beta_{bp} (I_1 + I_2 + I_3)_h; & h \text{ present} \\ 0; & \text{otherwise} \end{array} \right\} + \\ \left\{ \begin{array}{ll} \text{Bin}(S, 0.5); & j \text{ present, shares water-trough with } i, \text{ and FMDv load in 1 L of the water } \geq ID_{50} \text{ per oral} \\ 0; & \text{otherwise} \end{array} \right\} + \\ \left\{ \begin{array}{ll} \text{Bin}(S, 0.5); & h \text{ present, shares water-trough with } i, \text{ and FMDv load in 1 L of the water } \geq ID_{50} \text{ per oral} \\ 0; & \text{otherwise} \end{array} \right\} + \\ \left\{ \begin{array}{ll} \text{Bin}\left[\left(\frac{\text{FMDv_floor}_j \times \sigma}{ID_{50} \text{ per oral}}\right), 0.5\right]; & j \text{ present and } \left(\frac{\text{FMDv_floor}_j \times \sigma}{ID_{50} \text{ per oral}}\right) \leq S \\ 0; & \text{otherwise} \end{array} \right\} + \\ \left\{ \begin{array}{ll} \text{Bin}(S, p_{air_i}); & \sum_{k=1}^n I_3 \geq 0 \\ 0; & \text{otherwise} \end{array} \right\} - \delta L - \mu L$$

Subclinical infectious 1:

$$\frac{dI_1}{dt} = \delta L - \theta I_1 - \varphi I_1 + \varphi_{(t-1)} I_{1(t-1)} - \mu I_1$$

Subclinical infectious 2:

$$\frac{dI_2}{dt} = \theta I_1 - \varepsilon I_2 - \varphi I_2 + \varphi_{(t-1)} I_{2(t-1)} - \mu I_2$$

Clinical infectious:

$$\frac{dI_3}{dt} = \varepsilon I_2 - \gamma I_3 - (\varphi + \varsigma) I_3 + (\varphi_{(t-1)} + \varsigma) I_{3(t-1)} - (\mu + \psi) I_3$$

Clinical non-infectious:

$$\frac{dC}{dt} = \gamma I_3 - \tau C - (\varphi + \varsigma) C + (\varphi_{(t-1)} + \varsigma) C_{(t-1)} - (\mu + \psi) C$$

Recovered:

$$\frac{dR}{dt} = \tau C - \varphi R + \varphi_{(t-1)} R_{(t-1)} - \mu R$$

S-L Susceptible-Latent model of FMD infection dynamics in a hospital-pen 1

$$\frac{dS_{hpl}}{dt} = \sum_{i=1}^m \varphi S_i - \beta_{hp} \sum_{i=1}^m \varphi S_i \left[\sum_{i=1}^m \varphi I_{1i} + \sum_{i=1}^m \varphi I_{2i} + \sum_{i=1}^m (\varphi + \varsigma) I_{3i} \right]$$

$$\frac{dL_{hpl}}{dt} = \beta_{hp} \sum_{i=1}^m \varphi S_i \left[\sum_{i=1}^m \varphi I_{1i} + \sum_{i=1}^m \varphi I_{2i} + \sum_{i=1}^m (\varphi + \varsigma) I_{3i} \right]$$

TABLE 3 | Estimated percentage of latent cattle and home-pens with latent cattle on a U.S. beef cattle feedlot depending on the outbreak detection day since foot-and-mouth disease introduction.

Feedlot ^a	Percentage (%) of latent cattle and home-pens with latent cattle in the feedlot on the day of FMD outbreak detection (10th, 50th, 90th percentiles of $n = 2,000$ simulated outbreaks) ^b					
		Day 5	Day 6	Day 7	Day 8	Day 9
FS1	Cattle	<1, 4, 7	1, 10, 14	2, 14, 18	6, 18, 24	13, 24, 25
	Home-pens	25, 25, 25	25, 25, 30	25, 30, 41	25, 35, 50	25, 50, 65
FM1	Cattle	<1, 1, 2	0, 3, 4	1, 5, 5	3, 6, 6	4, 6, 7
	Home-pens	7, 7, 8	7, 7, 8	8, 10, 13	8, 12, 18	8, 15, 25
FM2	Cattle	<1, 1, 2	0, 3, 4	1, 5, 5	3, 6, 6	4, 6, 7
	Home-pens	7, 7, 8	7, 7, 8	8, 10, 13	8, 10, 15	8, 13, 18
FL1	Cattle	<1, 1, 1	0, 2, 2	1, 2, 3	1, 3, 3	2, 3, 4
	Home-pens	3, 3, 4	3, 3, 4	4, 4, 7	4, 5, 8	4, 7, 11
FL2	Cattle	<1, 1, 1	0, 2, 2	1, 2, 3	1, 3, 3	2, 3, 4
	Home-pens	3, 3, 3	3, 3, 4	4, 4, 7	4, 5, 8	4, 7, 9

^a Feedlot sizes and layouts modeled are detailed in **Table 2** and **Supplementary Figure 1**. Briefly, FS1 is a 4,000 cattle feedlot with one hospital-pen; FM1 is a 12,000 cattle feedlot with one hospital-pen; FM2 is a 12,000 cattle feedlot with two hospital-pens; FL1 is a 24,000 feedlot with two hospital-pens; and FL2 is a 24,000 cattle feedlot with four hospital-pens (in all the layouts $n = 200$ cattle per home-pen).

^b We show results of latent cattle and latent home-pens on days 5–9 (only) of outbreak detection on each feedlot size and layout modeled because those were the most common days of outbreak detection for the three detection thresholds modeled (3, 5, and 10% clinical cattle in the index home-pen).

TABLE 4 | Target parameters investigated for associations with the projected outbreak's peak day with highest number of clinical cattle since foot-and-mouth disease introduction and the total outbreak duration on a U.S. beef cattle feedlot.

Target parameter*	Parameter value distribution	Strength of the correlation (Spearman correlation coefficient value) between the model parameter value and outcome variable value for the feedlot of that size and layout									
		Peak day of the outbreak ^a					Duration of the outbreak				
		FS1 ^b	FM1	FM2	FL1	FL2	FS1	FM1	FM2	FL1	FL2
Beta transmission parameter in home-pens (β_{wp})	Triangular (0.02, 0.026, 0.031)	-0.14*	-0.21*	-0.09*	-0.09*	-0.10*	-0.05*	-0.08*	-0.14*	-0.09*	-0.08*
Bovine respiratory disease morbidity during the first 30 days of cattle placement in the feedlot (π)	Vector (0.05, 0.30, 0.05)	-0.01	-0.05	0.03	-0.10*	-0.17*	-0.05*	-0.13*	-0.15*	-0.07*	-0.05*
Depth of the home-pen floor top contaminated by fresh animal excreta (d_pen) (m)	Vector (2, 5, 3)	-0.06	-0.05	-0.01	-0.04	-0.03	-0.05	-0.05	-0.05	-0.06	-0.06
Initial proportion of latent cattle in the index home-pen ($lat_initial$)	Vector (0.005, 0.105, 0.020)	-0.42*	-0.29*	-0.09*	-0.15*	-0.17*	-0.11*	-0.09*	-0.08*	-0.09*	-0.09*
Fraction of saliva daily produced by the animal that is excreted into the home-pen environment (σ)	Vector (0.1, 0.5, 0.1)	0	-0.05	0.03	-0.05	-0.03	0.04*	0.03*	-0.01*	-0.01*	0.01*
Duration of FMD latent period (lat) (days)	Weibull ($\alpha = 1.782$, $\beta = 3.974$)	0.67*	0.62*	0.25*	0.48*	0.64*	0.75*	0.77*	0.77*	0.82*	0.83*
Duration of FMD infectious period (inf) (days)	Gamma ($\alpha = 3.969$, $\beta = 1.107$)	0.02	-0.11*	-0.02	-0.14*	-0.12*	0.48*	0.42*	0.23*	0.35*	0.29*
Duration of FMD subclinical period (sub) (days)	Gamma ($\alpha = 1.222$, $\beta = 1.672$)	0.19*	0.25*	0.07*	0.18*	0.22*	-0.21*	-0.17*	-0.03*	-0.09*	-0.06*
Water intake by the animal per visit to the water-trough in the home-pen (wat_int) (l)	Vector (1, 5, 4)	-0.02	-0.08	0.01	-0.09	-0.10	0.01	-0.01	-0.05	-0.06	-0.06

^a Bold coefficients with * indicate $p < 0.05$ for the correlation coefficient between the parameter value and outcome variable value.

^b Feedlot sizes and layouts modeled are detailed in **Table 2** and **Supplementary Figure 1**. Briefly, FS1 is a 4,000 cattle feedlot with one hospital-pen; FM1 is a 12,000 cattle feedlot with one hospital-pen; FM2 is a 12,000 cattle feedlot with two hospital-pens; FL1 is a 24,000 feedlot with two hospital-pens; and FL2 is a 24,000 cattle feedlot with four hospital-pens (in all the layouts $n = 200$ cattle per home-pen).

* Results of the following target parameters were not included in the table above because were found to be not influential to model outputs: mortality rate for animals with BRD and other production diseases (endemic infectious diseases and noninfectious diseases) (day^{-1}) (μ), Mortality rate for animals with clinical FMD (day^{-1}) (ψ), urine volume produced by an animal (L/day) (ur), saliva volume produced by an animal (L/day) (sal), volume of feces produced by an animal (kg/day) (fec), virus quantity shed in urine [plaque forming units (PFU)/mL] by an animal in the FMD clinical high infectious status ($uriv$), virus quantity shed in saliva (PFU/mL) by an animal in the FMD clinical high infectious status ($salv$), virus quantity shed in feces (PFU/mL) by an animal in the FMD clinical high infectious status ($fecv$), and the proportion of the cattle daily saliva volume deposited into the home-pen environment ($dmal$) ($fsal_env$). Their distributions can be found in **Table 1**.

Why it is important to incorporate space

Metapopulation models

A few foot-and-mouth disease models

Woolhouse and collaborators

Ringa & Bauch

Cabezas *et al*

Bradhurst *et al*

Buhnerkempe *et al*

Glass & Barnes

A few avian influenza models

A hybrid modeling approach to simulating foot-and-mouth disease outbreaks in Australian livestock

Richard A. Bradhurst^{1*}, Sharon E. Roche², Iain J. East², Paul Kwan¹ and M. Graeme Garner²

¹ Discipline of Computer Science, School of Science and Technology, University of New England, Armidale, NSW, Australia

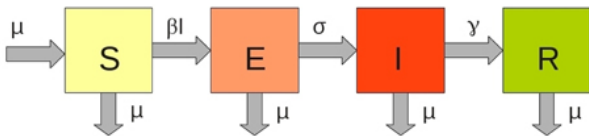
² Epidemiology and One Health Program, Animal Health Policy Branch, Department of Agriculture, Canberra, ACT, Australia

$$\frac{dS}{dt} = \mu - \beta IS - \mu S$$

$$\frac{dE}{dt} = \beta IS - \mu E - \sigma E$$

$$\frac{dI}{dt} = \sigma E - \mu I - \gamma I$$

$$\frac{dR}{dt} = \gamma I - \mu R$$



where S = proportion of the herd that are susceptible

E = proportion of the herd that are exposed

I = proportion of the herd that are infectious

R = proportion of the herd that are recovered

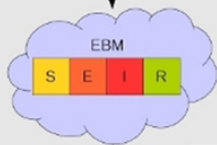
$\frac{1}{\mu}$ = average natural lifespan of the host, (μ = birth rate = natural mortality rate)

β = effective contact rate (contact rate \times transmission probability)

$\frac{1}{\sigma}$ = average duration of the latent period, (σ = progression rate from exposed to infectious)

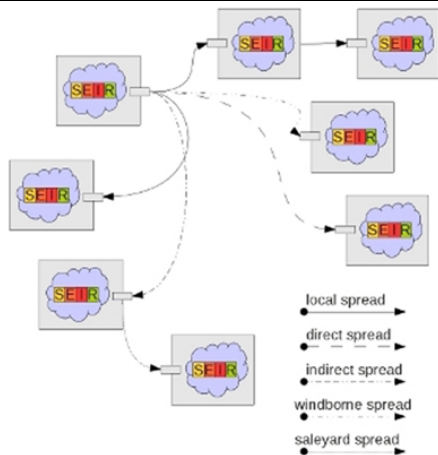
$\frac{1}{\gamma}$ = average duration of the infectious period, (γ = recovery rate)

- herd ID
- herd type (e.g. beef cattle)
- herd size
- farm location (lat/long)
- effective contact rate (β)
- incubation period ($1/\sigma$)
- infectious period ($1/\gamma$)
- clinical lag (days)
- initial conditions (s_0, e_0, i_0, r_0)



- compartment ratios(t)
- prevalence(t)
- clinical signs(t)

ABM interface



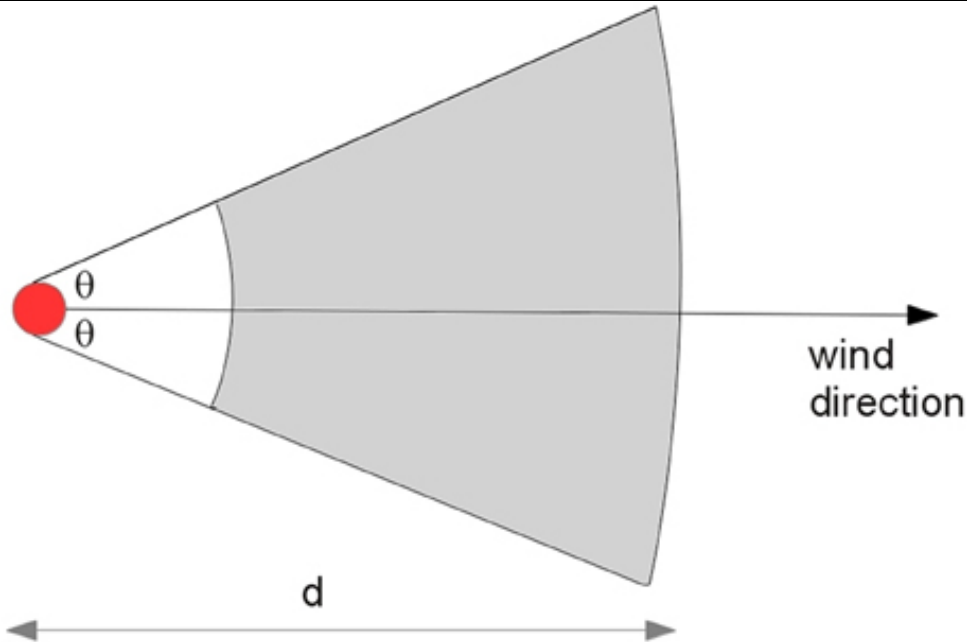


TABLE 1 | Herd and farm types used in AADIS.

Farm type	Number of farms	Mean farm population size (min–max)	Herd type	Number of herds
Extensive beef	1331	1909 (1200–46,575)	Extensive beef	3993
Intensive beef	51,383	280 (30 – 7436)	Intensive beef	51,383
Feedlot	508	1825 (100–39,963)	Feedlot	508
Mixed beef/sheep	21,556	242 (30 – 5700)	Mixed beef	21,556
			Mixed sheep	21,556
Dairy	8675	298 (40 – 2742)	Dairy	8675
Small pigs	1873	244 (40 – 4850)	Small pigs	1873
Large pigs	333	4922 (1000–17,896)	Large pigs	333
Sheep	22,150	1649 (20–44,000)	Sheep	22,150
Small holder	103,641	5 (1 – 14)	Small holder	103,641
Total	202,775			235,668

Why it is important to incorporate space

Metapopulation models

A few foot-and-mouth disease models

Woolhouse and collaborators

Ringa & Bauch

Cabezas *et al*

Bradhurst *et al*

Buhnerkempe *et al*

Glass & Barnes

A few avian influenza models

The Impact of Movements and Animal Density on Continental Scale Cattle Disease Outbreaks in the United States

Michael G. Buhnerkempe^{1*}†, Michael J. Tildesley², Tom Lindström³, Daniel A. Gear¹, Katie Portacci⁴, Ryan S. Miller⁴, Jason E. Lombard⁴, Marleen Werkman², Matt J. Keeling², Uno Wennergren³, Colleen T. Webb¹

1 Department of Biology, Colorado State University, Fort Collins, Colorado, United States of America, **2** Center for Complexity Science, Mathematics Institute, University of Warwick, Coventry, United Kingdom, **3** Department of Physics, Chemistry, and Biology, Linköping University, Linköping, Sweden, **4** United States Department of Agriculture, Animal and Plant Health Inspection Service, Centers for Epidemiology and Animal Health, Fort Collins, Colorado, United States of America

Table 1. Disease transmission routes in the model.

	Movement spread*	Non-movement spread	
		<i>Within-county</i>	<i>Local cross-border</i>
Cause	Animal Shipments	Aerosol, fence-line contact, or fomite transmission	Aerosol, fence-line contact, or fomite transmission
Spatial Scale	All counties in the US	Premises within an infected county	All neighboring counties
Assumptions	1) Premises density-dependent; 2) Spatially explicit [†] ; 3) Differs by state and production type	1) Premises density-dependent; 2) Premises size dependent	1) Premises density-dependent [‡] ; 2) Premises size dependent [‡] ; 3) Spatially implicit [§]
Informed by or data from	1) ICVI records; 2) Number of premises by county and production type [¶] ; 3) State cattle inflows [38]	1) 2001 UK FMD outbreak [39]; 2) US premises density and size distributions [¶]	1) 2001 UK FMD outbreak [39]; 2) US premises density and size distributions [¶] ; 3) Shared county border length
Parameter Uncertainty	Estimated through Bayesian inference and incorporated in the simulations via multiple realizations of shipment networks.	Broad parameter ranges explored in a sensitivity analysis .	Broad parameter ranges explored in a sensitivity analysis .

*See Section C in Text S1 and Lindström et al. [24].

[†]Based on county centroids.

[‡]In both the focal and neighboring counties.

[§]Based on randomly distributed premises in the focal and neighboring counties.

[¶]See Section B in Text S1 and NASS census data [15].

^{||}See Section E in Text S1.

doi:10.1371/journal.pone.0091724.t001

Table 2. Disease simulation model parameters.

Type	Parameter	Value	Range	Description
Transmission	β	0.0003508 [*]	[2×10^{-5} , 4×10^{-2}]	Transmission rate between cattle on different premises
	α	4.6 [†]	[2.1, 6]	Shape of the local, non-movement spatial kernel
	θ	1.6 [‡]	[1,6]	Scale of the local, non-movement spatial kernel
	p	0.414 [†]	[0, 1]	Non-linear scaling of the effect of premises size (i.e., number of cattle) on susceptibility to infection
	q	0.424 [†]	[0, 1]	Non-linear scaling of the effect of premises size (i.e., number of cattle) on transmission of infection
Control	ε	100% [†]	[50%,100%]	Percentage of movements to/from an area that are stopped by a movement ban
	λ	7 [§]	7, 14, 21	The delay between a premises becoming infected and subsequently being identified and removed, which triggers movement bans
Other	σ	5 [§]	NA [¶]	The latent period; amount of time between a premises being exposed to infection and becoming infectious

*Units in Premises (days)⁻¹.

[†]Unit-less parameter.

[‡]Units in kilometers.

[§]Units in days.

[¶]Sensitivity analysis was not performed on this parameter.

doi:10.1371/journal.pone.0091724.t002

A**B**

Figure 1. State-to-state cattle flows. Given for the (A) ERS ICVI summary data [16] and (B) 10% sample of paper ICVIs.
doi:10.1371/journal.pone.0091724.g001



**Figure 2. The giant strongly connected component (GSCC) of the network from a 10% sample of ICVis. Maps at the (A) state and (B) county scales. Orange denotes a node in the GSCC. Brown denotes a node outside of the GSCC that either sends to or receives from nodes in the GSCC but not both, and black indicates nodes that are isolated from the GSCC. Gray indicates no data. New Jersey is outside GSCC because it was the only state not to supply ICVI d
doi:10.1371/journal.pone.0091724.g002**

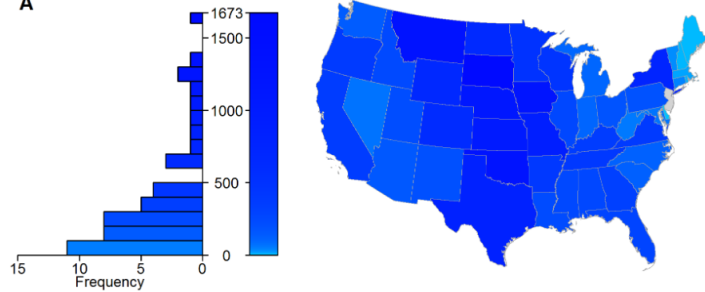
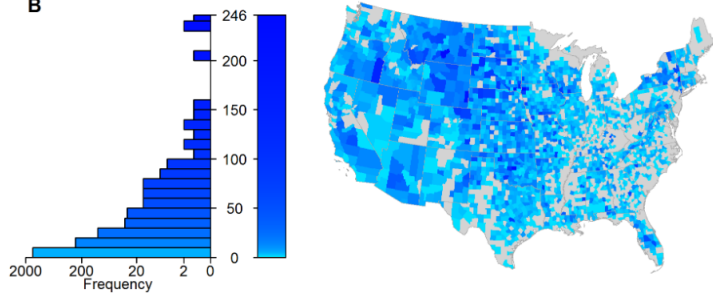
A**B**

Figure 3. Out-degree distributions of the cattle movement network from a 10% sample of ICVIs. The network is aggregated into (A) state and (B) county nodes. The left-hand graphs show the frequency distribution of node out-degrees, while the maps show the value for that area. A logarithmic color scale is used to differentiate high (dark blue) from low (light blue) out-degree. Counties with no sampled out-shipments are indicated in gray.

doi:10.1371/journal.pone.0091724.g003

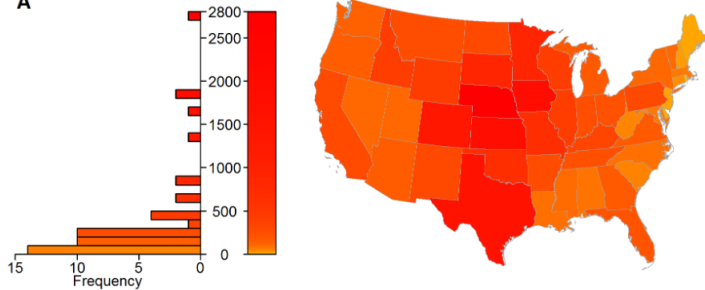
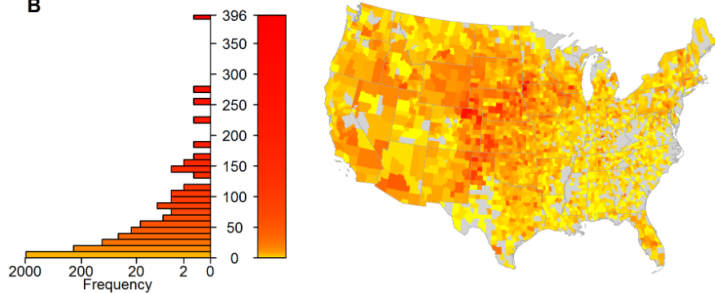
A**B**

Figure 4. In-degree distributions of the cattle movement network from a 10% sample of ICVIs. The network is aggregated into (A) state and (B) county nodes. The left-hand graphs show the frequency distribution of node in-degrees, whilst the maps show the value for that area. A logarithmic color scale is used to differentiate high (red) from low (yellow) in-degree. Counties with no sampled in-shipments are indicated in gray.

doi:10.1371/journal.pone.0091724.g004

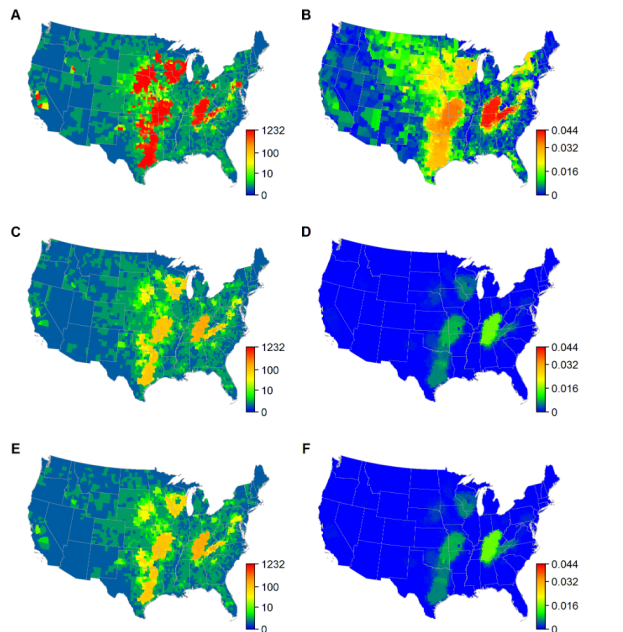


Figure 5. Epidemic extent and infection risk with unrestricted, county and, state movement bans. Upper tail of the distribution (based on the 97.5th percentile of 100 simulations) for epidemic extent and infection risk when infections are introduced to each of the 3109 counties of the continental US. (A & B) assume standard movements while (C & D) assume a county-level movement ban and (E & F) assume a state-level movement ban. (A, C, & E) the epidemic extent (the number of counties infected) for an infection seeded in each county. (B, D, & F) the infection risk (the proportion of all simulated outbreaks that infect a county).

doi:10.1371/journal.pone.0091724.g005

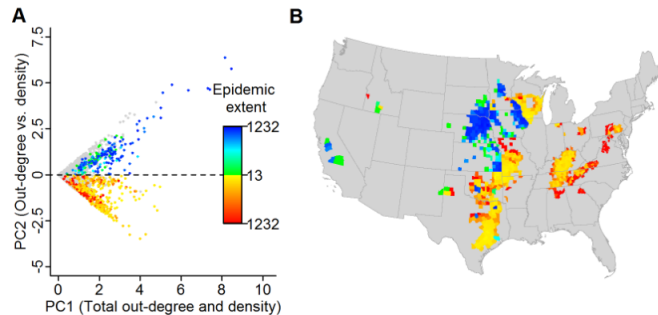


Figure 6. Relative importance of movement vs. local spread determined through a Principal component analysis. (A) Plot of PC1 ($0.7071 \cdot \text{Out-degree} + 0.7071 \cdot \text{Premises density}$) vs. PC2 ($0.7071 \cdot \text{Out-degree} + 0.7071 \cdot \text{Premises density}$) for each county. Colored dots represent counties in the upper 20% of simulated epidemic extents with the counties where movement is relatively more important (i.e., $\text{PC2} > 0$) ranging from green to blue and the counties where density is relatively more important (i.e., $\text{PC2} < 0$) ranging from yellow to red based on epidemic extent. (B) Map depicting the spatial distribution of the counties within the upper 20% of epidemic extents.

doi:10.1371/journal.pone.0091724.g006

Why it is important to incorporate space

Metapopulation models

A few foot-and-mouth disease models

Woolhouse and collaborators

Ringa & Bauch

Cabezas *et al*

Bradhurst *et al*

Buhnerkempe *et al*

Glass & Barnes

A few avian influenza models



Eliminating infectious diseases of livestock: A metapopulation model of infection control



Kathryn Glass*, Belinda Barnes

National Centre for Epidemiology and Population Health, Australian National University, Canberra, Australia

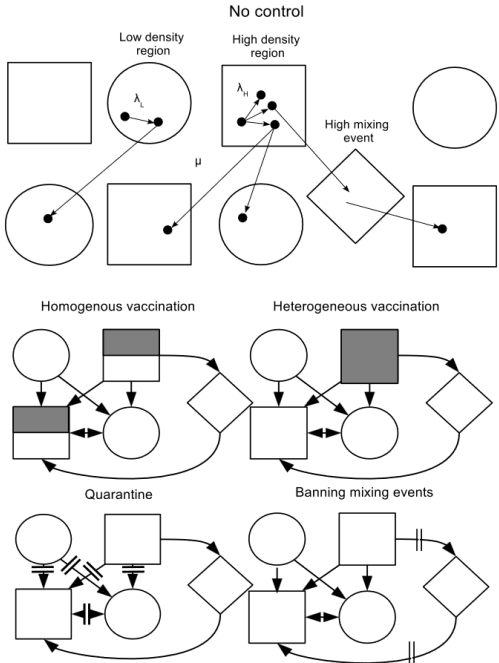


Fig. 1. Diagram of the model with and without control. Squares represent high-density regions (with local mixing rate λ_H), and circles represent low-density regions (with local mixing rate λ_L). Between-region mixing occurs according to a rate μ , as well as through high-mixing events or locations (diamond). Four control measures are shown: homogenous vaccination of high-density regions, heterogeneous vaccination of high-density regions, quarantine, and banning of high-mixing events.

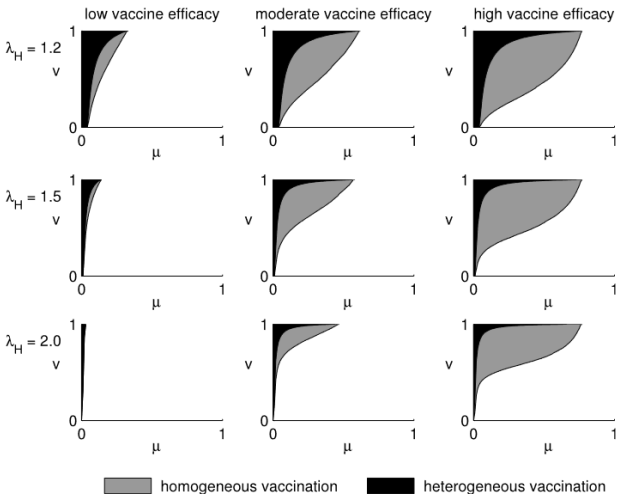


Fig. 2. The regions of parameter space for which disease can be eliminated by homogeneous and heterogeneous vaccination. Each plot shows a shaded region in μ - v space giving parameter combinations for which disease is eliminated, where μ is the between-region transmission parameter, and v is the vaccine coverage. That is, $v = v$ for homogeneous vaccination, and $v = V$ for heterogeneous vaccination. Note that regions are nested, so that the darkest region represents areas of parameter space where both interventions are successful. We consider three different values for the within-region transmission parameter in high-density regions ($\lambda_H = 1.2, 1.5, 2.0$), represented by the three rows of the figure. Vaccine efficacy can be low ($\alpha_l = \alpha_s = \sqrt{0.7}$), medium ($\alpha_l = \alpha_s = \sqrt{0.4}$), or high ($\alpha_l = \alpha_s = \sqrt{0.1}$), as shown in the three columns of the figure. We assume the transmission parameter for low-density regions is fixed at $\lambda_L = 0.6$, and set $n = 400$ and $\pi = 0.5$.

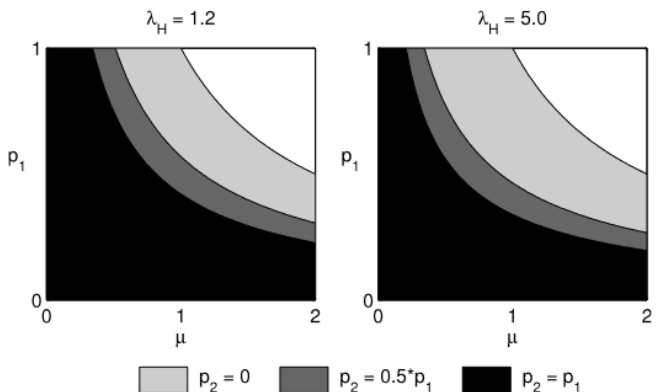


Fig. 3. The regions of parameter space for which disease can be eliminated by reactive quarantine according to the extent that quarantine reduces transmission from the first and second generation of cases. Each plot shows a shaded region in μ - p_1 space giving parameter combinations for which disease is eliminated, where μ is the between-region transmission parameter, and p_1 is the proportion of the primary case's infectivity that occurs before quarantine is in place. Note that regions are nested, so that the darkest region represents areas of parameter space where all interventions are successful. We compare two extreme values for the within-region transmission parameter in high-density regions ($\lambda_H = 1.2, 5.0$), represented by the two subplots in the figure. The different regions (black, dark grey and light grey) compare the proportion of infectivity experienced by secondary cases (p_2). We assume the transmission parameter for low-density regions is fixed at $\lambda_L = 0.6$, and set $n = 400$ and $\pi = 0.5$.

Why it is important to incorporate space

Metapopulation models

A few foot-and-mouth disease models

A few avian influenza models

Andronico et al

Why it is important to incorporate space

Metapopulation models

A few foot-and-mouth disease models

A few avian influenza models

Andronico et al



Highly pathogenic avian influenza H5N8 in south-west France 2016–2017: A modeling study of control strategies



Alessio Andronico^{a,*}, Aurélie Courcoul^{b,1}, Anne Bronner^c, Axelle Scoizec^d,
Sophie Lebouquin-Leneveu^d, Claire Guinat^e, Mathilde C. Paul^e, Benoît Durand^b,
Simon Cauchemez^a

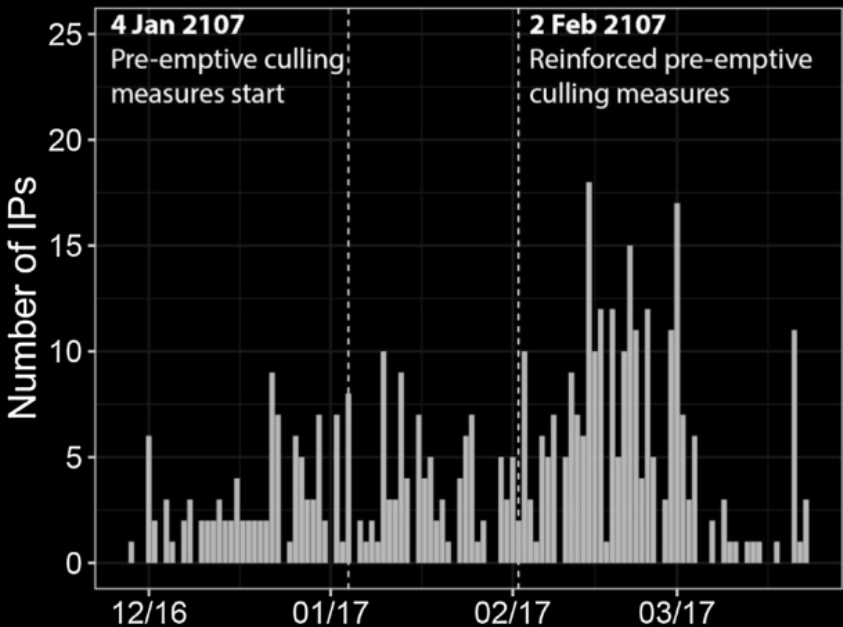
^a Mathematical Modelling of Infectious Diseases Unit, Institut Pasteur, UMR2000, CNRS, 75015, Paris, France

^b Epidemiology Unit, Paris-Est University, Laboratory for Animal Health, French Agency for Food, Environment and Occupational Health and Safety (ANSES), Maisons-Alfort, France

^c Direction générale de l'Alimentation, Paris, 75015, France

^d Anses, Laboratoire de Ploufragan-Plouzané, Unité d'épidémiologie et bien-être en aviculture et cuniculture, Ploufragan, 22440, France

^e IHAP, Université de Toulouse, INRA, ENVT, Toulouse, France



A metapopulation model for highly pathogenic avian influenza: implications for compartmentalization as a control measure

S. NICKBAKHS¹, L. MATTHEWS¹, S. W. J. REID² AND R. R. KAO^{1*}

¹ Institute of Biodiversity, Animal Health and Comparative Medicine, University of Glasgow, Bearsden Road, Scotland, UK

² Royal Veterinary College, University of London, North Mymms, Hatfield, Hertfordshire, UK

Received 4 July 2013; Final revision 18 October 2013; Accepted 30 October 2013;
first published online 5 December 2013

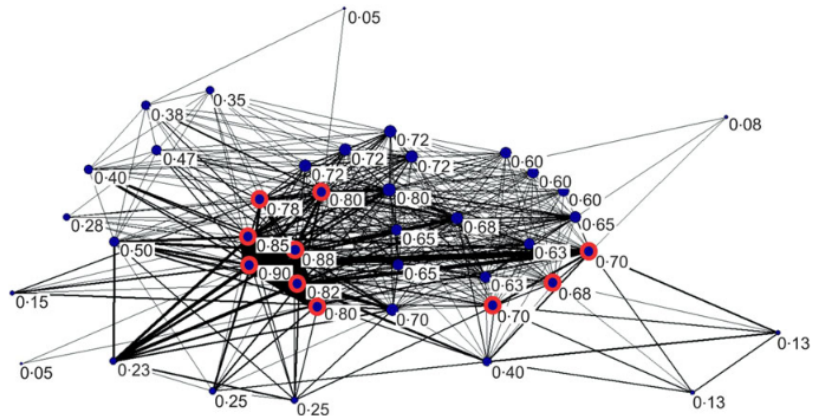


Fig. 1 [colour online]. Unipartite representation of the poultry company network of associations via slaughterhouses and catching companies; $n=41$ poultry companies (excluding four that were unconnected to the giant component). Node labels are the normalized (by largest possible value) degree centralities with relative magnitudes represented by node size. Nodes circled in red represent companies which also had a relatively high betweenness centrality. The line widths represent the number of slaughterhouses and/or catching companies that formed the associations.

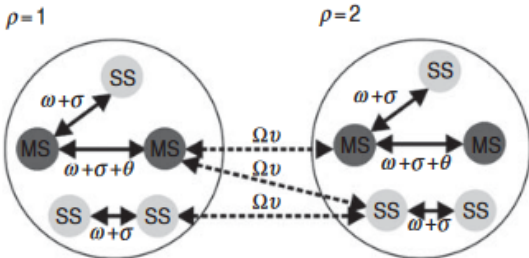


Fig. 2. Schematic of the metapopulation model. The compartment populations represent the multi-site (MS) premises associated with a company from the network *core* ($\rho=1$) and the network *periphery* ($\rho=2$), and the single-site (SS) premises within proximity. Solid arrows = within-population links; dashed arrows = between-population links; Ω = between-population network link weights; v = between-population interaction strength; ω = within-population network link weights; θ = company-related network link weights and σ = within-population spatial link weights. See [Table 1](#) for full parameter details. Note that this schematic does not reflect the actual relative numbers of MS and SS premises assumed in these analyses.

The baseline model for the interaction between population 1 (network *core* group) and population 2 (network *periphery* group) is described by the following set of ordinary differential equations:

$$\frac{dS_{pj}}{dt} = -S_{pj}(W_{pj} + B_{pj}),$$

$$\frac{dI_{pj}}{dt} = S_{pj}(W_{pj} + B_{pj}) - \gamma I_{pj},$$

$$\frac{dR_{pj}}{dt} = \gamma I_{pj},$$

where $\rho=\{1, 2\}$ for population 1 (network *core*) and population 2 (network *periphery*) and $j=\{\text{MS, SS}\}$ for multi-site and single-site premises types and $W_{\rho j}$ and $B_{\rho j}$ represent the within- and between-population forces of infection acting upon premises type j within population ρ .

The force of infection acting on $j=MS$ premises within $\rho=1$ (network core group) is further deconstructed as follows:

$$W_{1,MS} = \beta \left(\omega_{MS,MS} \frac{I_{1,MS}}{n_{1,MS}} + \omega_{MS,SS} \frac{I_{1,SS}}{n_{1,SS}} \right)$$

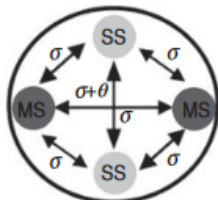
$$+ \beta'_{1,MS} \left(\sigma_{MS,MS} \frac{I_{1,MS}}{n_{1,MS}} + \sigma_{MS,SS} \frac{I_{1,SS}}{n_{1,SS}} \right)$$

$$+ \beta \left(\theta \delta_{MS,1} \frac{I_{1,MS}}{n_{1,MS}} \right)$$

$$B_{1,\text{MS}} = \beta \left(\Omega_{\text{MS},\text{MS}} v \frac{I_{2,\text{MS}}}{n_{2,\text{MS}}} \right) + \beta \left(\Omega_{\text{MS},\text{SS}} v \frac{I_{2,\text{SS}}}{n_{2,\text{SS}}} \right),$$

where β and $\beta'_{1,\text{MS}}$ are density-independent and density-dependent transmission rates (days^{-1}), respectively, $\sigma_{\text{MS},k}$ and $\omega_{\text{MS},k}$ weight the rate of transmission from premises type $k=\{\text{MS, SS}\}$ to MS premises through spatial proximity and network links respectively, θ weights the rate of transmission between MS premises of the same company, $\delta_{\text{MS},1}$ is the Kronecker delta function, where $\delta_{jk}=1$ if $j=\text{MS}$ premises or zero otherwise, $\Omega_{\text{MS},k}$ weights the rate of transmission between populations and v is a uniform weighting applied to $\Omega_{\text{MS},k}$ in order to vary the relative strength of transmission between populations (i.e. the interaction, or coupling, strength). These equations can equivalently represent the force of infection acting on SS premises by substituting $j=\text{SS}$ premises and for population 2 by substituting $\rho=2$.

(a) Compartmentalization



(b) Zoning

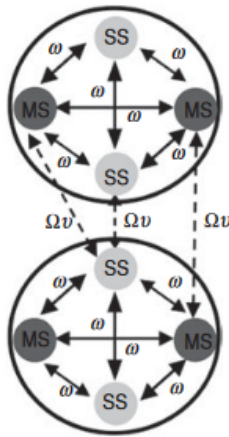


Fig. 4. Schematic representation of zoning and compartmentalization control scenarios. (a) Under compartmentalization the following links were enabled: spatial and within-company links (σ, θ). (b) Under zoning control the following links were enabled: within-population network-mediated links (beyond 10 km) and between-population network links ($\omega, \Omega v$).

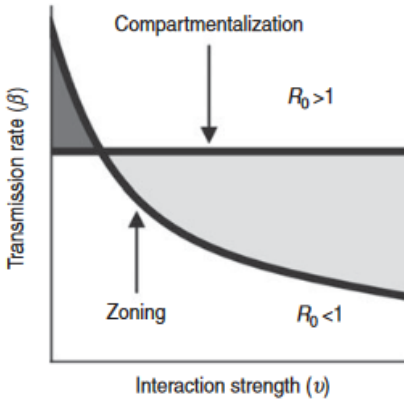


Fig. 7. Schematic representation of the relative risk of infection spillover under compartmentalization. Dark-shaded area represents the additional risk of an outbreak (where $R_0 > 1$) under compartmentalization and light-shaded area represents the additional risk of an outbreak (where $R_0 > 1$) under zoning. The relative risk under compartmentalization can be increased through two ways: (i) a rightwards shift to the curve under zoning or (ii) a downwards shift to the line under compartmentalization.

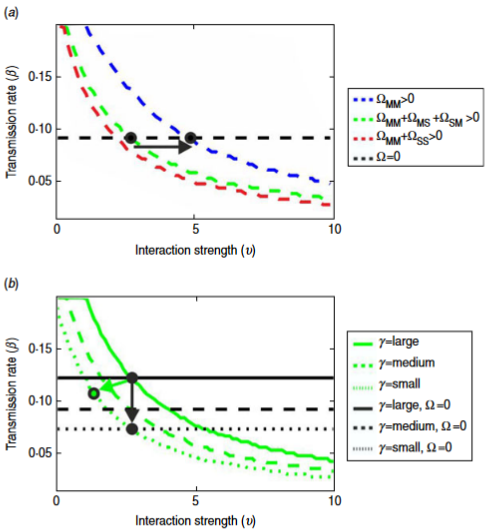


Fig. 8. R_0 thresholds under zoning (coloured curves) vs. compartmentalization (black lines). Ω_{MM} =links between multi-site premises, Ω_{MS} and Ω_{SM} =links between multi-site and single-site premises; Ω_{SS} =links between single-site premises. (a) For a medium infectious period corresponding to a premises depopulation rate of $0.25 (\text{day}^{-1})$, relative risk under compartmentalization was increased when the links enabling between-population interaction were reduced (from red to green to blue), as indicated by the arrow. Link types not shown in the legend are switched-off (i.e. $\Omega=0$). (b) For between-population interactions involving multi-site and single-site premises (i.e. Ω_{MS} , Ω_{SM} , Ω_{SS}), the relative risk increased with the infectious period (from solid to dotted lines) under compartmentalization (black arrow) and zoning (green arrow). This model scenario assumed density-dependent spatial transmission occurred within a distance radius of 1 km.

Impact of the implementation of rest days in live bird markets on the dynamics of H5N1 highly pathogenic avian influenza

G. Fournié^{1,*}, F. J. Guitian¹, P. Mangtani² and A. C. Ghani³

¹ Veterinary Epidemiology and Public Health Group, Department of Veterinary Clinical Sciences, Royal Veterinary College, London, UK

² Infectious Disease Epidemiology Unit, London School of Hygiene and Tropical Medicine, London, UK

³ MRC Centre for Outbreak Analysis and Modelling, Department of Infectious Disease Epidemiology, Imperial College London, London, UK

Infectious birds are assumed to contaminate their environment by releasing faeces at each time step. Faeces infectiousness decreases exponentially with time at a rate Θ . Therefore, during the infectious period of a bird, disease is transmitted directly through contact with susceptible birds and indirectly through the contaminated environment (figure 1b). Transmission continues after the death of the infectious bird via the remaining environmental reservoir. The infectiousness via each route of transmission can therefore be expressed as:

$$\text{inf}_{\text{contact}} = \int_{t=0}^{t=T_{\text{inf}}} \beta dt = \beta T_{\text{inf}}, \quad (2.1)$$

$$\begin{aligned} \text{inf}_{\text{env}} &= \int_{t=0}^{t=T_{\text{inf}}} dt \int_{t=0}^{t=H} \beta \eta (1 - \Theta)^t dt \\ &= T_{\text{inf}} \int_{t=0}^{t=H} \beta \eta (1 - \Theta)^t dt, \end{aligned} \quad (2.2)$$

where T_{inf} is the infectious period, H is the length of time the faeces remains infectious, β is the per unit time rate of transmission and η the relative rate of transmission from the environmental reservoir compared with β . In equation (2.2), the integral refers to the exponential decay of faeces dropped each day that the bird is infectious, which extends the infectious period in the environment beyond the infectious

period of the bird. For a stable population size and an infectious period going to its end without being stopped owing to selling and slaughtering, the basic reproduction number R_0 (i.e. expected number of secondary cases following the introduction of a primary case in a susceptible population) is then defined as:

$$R_0 = (\inf_{\text{contact}} + \inf_{\text{env}}) N_0, \quad (2.3)$$

where N_0 is the initial number of susceptible birds in the market. We can thus define the environmental contamination ratio ζ as the proportion of infectivity, which is mediated by the environment:

$$\zeta = \frac{\inf_{\text{env}} N_0}{R_0} = \frac{\beta \eta T_{\text{inf}} N_0}{R_0} \int_{t=0}^{t=H} (1 - \Theta)^t dt. \quad (2.4)$$

Thus, knowing ζ and R_0 , we can calculate β and η :

$$\beta = \frac{R_0}{T_{\text{inf}} N_0 (1 + \eta \int_{t=0}^{t=H} (1 - \Theta)^t dt)} \quad (2.5)$$

$$\eta = \frac{\zeta}{(1 - \zeta)} \frac{1}{\int_{t=0}^{t=H} (1 - \Theta)^t dt}. \quad (2.6)$$

The infection process is stochastic and density-dependent. Homogeneous mixing is assumed.

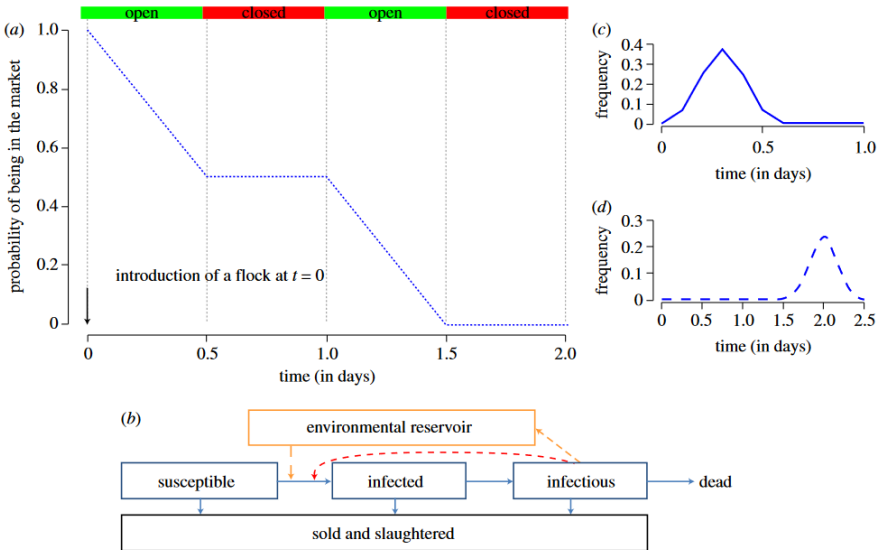


Figure 1. Illustration of the within-market model. (a) Probability that a bird introduced at time $t = 0$ remains in the market as a function of time. In green: period during which the market is open for trading. In red: period during which the market is closed for trading. (b) Within-market SEI model. (c) Assumed distribution of the latent period (solid line, latent period). (d) Assumed distribution of the infectious period (dotted line, infectious period).

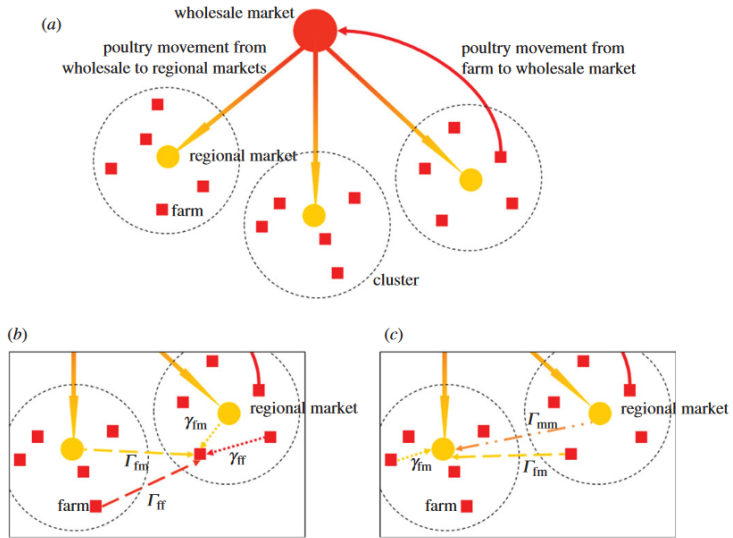


Figure 2. Diagram of the poultry sector and routes of disease transmission in the meta-population model. (a) Diagram of the poultry sector. All farms (red square) are clustered around regional markets (yellow circle). Poultry movements are from farms to the wholesale market (red circle) and from the wholesale to the retail markets. (b) A given farm can be infected by farms located in the same cluster (red dotted arrow, relative strength of mixing: γ_{ff}), by farms in other clusters (red dashed arrow, Γ_{ff}), by a market in the same cluster (yellow dotted arrow, γ_{fm}) and by markets in other clusters (yellow dashed arrow, Γ_{fm}). (c) A given regional market can be infected by the introduction of infected birds from the wholesale market, ^{b,w} markets in other clusters (orange dotted-dashed arrow, Γ_{mm}), by farms in the same cluster (yellow dotted arrow, γ_{fm}) and farms in other clusters (yellow dashed arrow, Γ_{ff}).

In farm i in cluster j with $S_{i,j}^F(t)$ susceptible birds at time t , the number of newly infected birds at $t + dt$ is given by a stochastic binomial variable $B(\lambda_{i,j}^F(t), S_{i,j}^F(t))$, where $\lambda_{i,j}^F(t)$ is the force of infection (i.e. the rate at which poultry gets infected between t and $t + dt$) defined by:

$$\lambda_{i,j}^F(t) = 1 - \exp\left\{-\delta_{i,j}^F(t)dt\right\}. \quad (2.7)$$

Here $\delta_{i,j}^F(t)$ is the instantaneous hazard of infection:

$$\begin{aligned} \delta_{i,j}^F(t) &= \beta^F \left[I_{i,j}^F(t) + \eta^F \psi_{i,j}^F(t) \right] + \left[\gamma_{ff} \sum_{l \neq j} \psi_{i,l}^F(t) \right] \\ &\quad + \left[\Gamma_{ff} \sum_{k \neq i, l} \psi_{k,l}^F(t) \right] + [\gamma_{fm} \psi_i^M(t)] + \left[\Gamma_{fm} \sum_{k \neq i} \psi_k^M(t) \right] \end{aligned} \quad (2.8)$$

Similarly in a regional market i :

$$\lambda_i^M(t) = 1 - \exp\{-\delta_i^M(t)dt\}, \quad (2.9)$$

with the hazard of infection $\delta_i^M(t)$ given by:

$$\begin{aligned}\delta_i^M(t) = & \beta^M [I_i^M(t) + \eta^M \psi_i^M(t)] + \left[\gamma_{fm} \sum_l \psi_{i,l}^F(t) \right] \\ & + \left[\Gamma_{fm} \sum_{k \neq i, l} \psi_{k,l}^F(t) \right] + \left[\Gamma_{mm} \sum_{k \neq i} \psi_k^M(t) \right].\end{aligned}\quad (2.10)$$

Here the first component is the within-market infection process, the second the hazard of infection from farms in the same cluster, the third from farms in other clusters and the fourth from markets in other clusters.

At the wholesale market, the force of infection is assumed to depend only on within-market infection process.

We assume that $\Gamma_{fm} = \Gamma_{mm}$ and $\gamma_{ff}/\gamma_{fm} = \Gamma_{ff}/\Gamma_{fm}$.

Both models were implemented in BERKELEY MADONNA v. 8.4.14 [28].

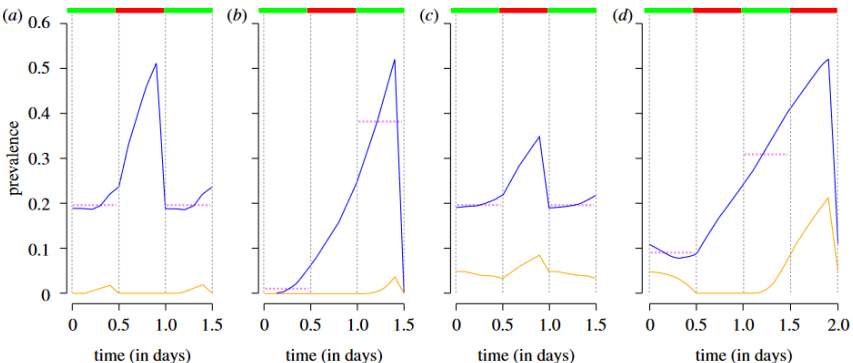


Figure 3. Prevalence of infectious and symptomatic birds in the market under four different scenarios. (a) $T_r = 1.5$ days, introduction of a cohort every day. (b) $T_r = 1.5$ days, introduction of a cohort every 2 days. (c) $T_r = 2.5$ days, introduction of a cohort every day. (d) $T_r = 2.5$ days, introduction of a cohort every 2 days. In all scenarios the mean prevalence P^m is 19.5%, the corresponding reproduction number R_0^m assuming the same β and η is equal to (a) 16.8, (b) 35.1, (c) 6.4, (d) 9.2. Each graph shows the mean prevalence of infectious birds at each time step (solid blue line), the mean prevalence of infectious birds during the open period (dotted violet line) and the mean prevalence of symptomatic birds for each time step (solid orange line). 95% bounds from the stochastic realizations closely follow the mean and so are not presented.

RESEARCH ARTICLE

Effective control measures considering spatial heterogeneity to mitigate the 2016–2017 avian influenza epidemic in the Republic of Korea

Jonggul Lee¹, Youngsuk Ko², Eunok Jung^{2*}

1 National Institute for Mathematical Sciences, Daejeon, Republic of Korea, **2** Mathematic department, Konkuk University, Seoul, Republic of Korea

* junge@konkuk.ac.kr



Abstract

During the winter of 2016–2017, an epidemic of highly pathogenic avian influenza (HPAI) led to high mortality in poultry and put a serious burden on the poultry industry of the Republic of Korea. Effective control measures considering spatial heterogeneity to mitigate the HPAI epidemic is still a challenging issue. Here we develop a spatial-temporal compartmental model that incorporates the culling rate as a function of the reported farms and farm density in each town. The epidemiological and geographical data of two species, chickens and ducks, from the farms in the sixteen towns in Eumseong-gun and Jincheon-gun are used to find the best-fitted parameters of the metapopulation model. The best culling radius to maxi-

OPEN ACCESS

Citation: Lee J, Ko Y, Jung E (2019) Effective control measures considering spatial heterogeneity to mitigate the 2016–2017 avian influenza epidemic in the Republic of Korea. PLoS ONE 14(6): e0218202. <https://doi.org/10.1371/journal.pone.0218202>

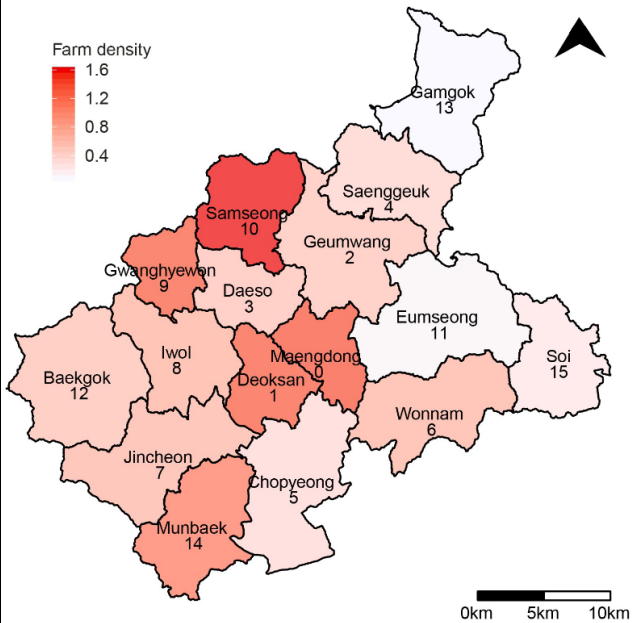


Fig 1. Map of Eumseong-gun and Jincheon-gun, which are the municipal-level divisions located in the central part of the Republic of Korea, including the density of poultry farms with white indicating low density and red indicating high density. The index of the town is written below its name. There are 16 towns; 9 towns in Eumseong-gu and 7 in Jincheon-gu. Reprinted from [27] under a CC BY license, with permission from National Geographic Information Institute, original copyright 2017.

Metapopulation model with two species

Now we consider a compartmental model to incorporate spatial effects. Let S_i, I_i, R_i denote respectively the number of susceptible, infective but not identified, and reported farms in patch i for $i = 0, \dots, 15$. Note that in our model I_i and R_i are infectious, but R_i has less transmissibility because of control measures after the case is identified, such as isolation and restriction. Ignoring the species, the spatial-temporal model can be written for $i = 0, \dots, 15$ as follows

$$\begin{aligned}\frac{dS_i}{dt} &= -\sum_{j=0}^{15} \beta(I_j + \epsilon R_j) K(i,j) S_i - \psi(R_i, D_i; \mathbf{R}) S_i, \\ \frac{dI_i}{dt} &= \sum_{j=0}^{15} \beta(I_j + \epsilon R_j) K(i,j) S_i - \alpha I_i - \psi(R_i, D_i; \mathbf{R}) I_i, \\ \frac{dR_i}{dt} &= \alpha I_i - \phi(\mathbf{R}) R_i,\end{aligned}\tag{1}$$

$$\text{where } K(i,j) = e^{-\frac{d(i,j)}{\tau_0}}.$$

We now introduce a metapopulation model with two-type poultry farms: chicken and duck. For $i = 0, \dots, 15$, S_i , I_i and R_i are divided into two poultry farms such as S_{ci} , I_{ci} , R_{ci} , S_{di} , I_{di} and R_{di} , respectively, where the subscript c is for chicken and d for duck. Then the model with two different farms can be written for $i = 0, \dots, 15$ as the following nonlinear differential equations:

$$\begin{aligned} \frac{dS_{ci}}{dt} &= -\sum_{j=0}^{15} \left(\beta_{cc}(I_{cj} + \epsilon R_{cj}) + \beta_{cd}(I_{dj} + \epsilon R_{dj}) \right) K(i, j) S_{ci} - \psi(R_i, D_i; \mathbf{R}) S_{ci}, \\ \frac{dI_{ci}}{dt} &= \sum_{j=0}^{15} \left(\beta_{cc}(I_{cj} + \epsilon R_{cj}) + \beta_{cd}(I_{dj} + \epsilon R_{dj}) \right) K(i, j) S_{ci} - \alpha_c I_{ci} - \psi(R_i, D_i; \mathbf{R}) I_{ci}, \\ \frac{dR_{ci}}{dt} &= \alpha_c I_{ci} - \phi(\mathbf{R}) R_{ci}, \\ \frac{dS_{di}}{dt} &= -\sum_{j=0}^{15} \left(\beta_{dc}(I_{cj} + \epsilon R_{cj}) + \beta_{dd}(I_{dj} + \epsilon R_{dj}) \right) K(i, j) S_{di} - \psi(R_i, D_i; \mathbf{R}) S_{di}, \tag{2} \\ \frac{dI_{di}}{dt} &= \sum_{j=0}^{15} \left(\beta_{dc}(I_{cj} + \epsilon R_{cj}) + \beta_{dd}(I_{dj} + \epsilon R_{dj}) \right) K(i, j) S_{di} - \alpha_d I_{di} - \psi(R_i, D_i; \mathbf{R}) I_{di}, \\ \frac{dR_{di}}{dt} &= \alpha_d I_{di} - \phi(\mathbf{R}) R_{di}, \end{aligned}$$

where $K(i, j) = e^{-\frac{d(i,j)}{r_0}}$.

Reproductive numbers

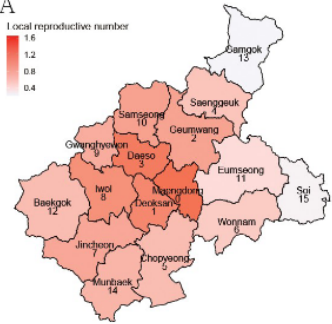
When an infected individual invades the susceptible population, the average number of secondary infection generated by the primary case over the infectious period, called the *basic reproductive number* and denoted by \mathcal{R}_0 , is an important threshold quantity [31–33]. In this work, to find the basic reproductive number, we use the next generation method [33, 34]. Let \mathbf{G} be the next generation matrix, then $\mathcal{R}_0 = \rho(\mathbf{G})$ where ρ is the spectral radius. The (i, j) element of \mathbf{G} means how many new infections are introduced into compartment i by the infected from compartment j . We now define the *local* reproductive number in town j , $\mathcal{R}_0^{(j)}$, as how many poultry farms are newly infected by infected poultry farms from town j , and it is obtained by the maximum value among the farming types in each town after the sum of each column of \mathbf{G} . As we consider two types of poultry farms, the next generation matrix can be written as a 2×2 block matrix,

$$\mathbf{G} = \left[\begin{array}{c|c} G_{cc} & G_{cd} \\ \hline G_{dc} & G_{dd} \end{array} \right] \quad (3)$$

where the block $G_{k_1 k_2}$ for $k_1, k_2 \in \{c, d\}$ is a 16×16 matrix, and the entry of $G_{k_1 k_2}$ is given by

$$G_{k_1 k_2}[i, j] = \beta_{k_1 k_2} S_{k_1 i}(0) \left(\frac{1}{\alpha_{k_2}} + \frac{\epsilon}{\gamma} \right) K(i, j). \quad (4)$$

A



B

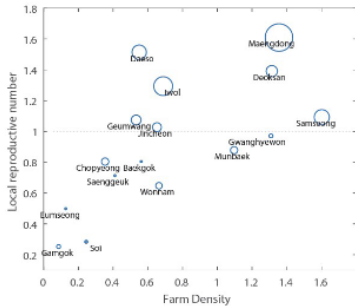


Fig 4. (A) Local reproductive numbers in each town. The darker red color represents the larger reproductive number. (B) Local reproductive number with respect to farm density in each town. The size of circle shows the size of duck farms. Reprinted from [27] under a CC BY license, with permission from National Geographic Information Institute, original copyright 2017.

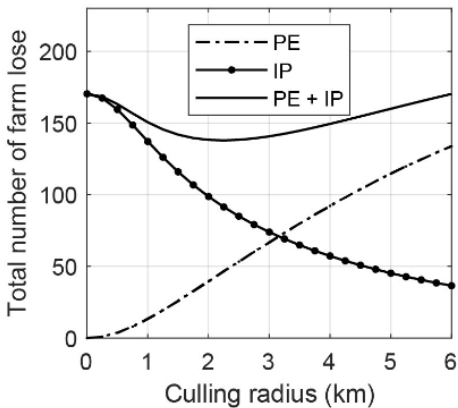
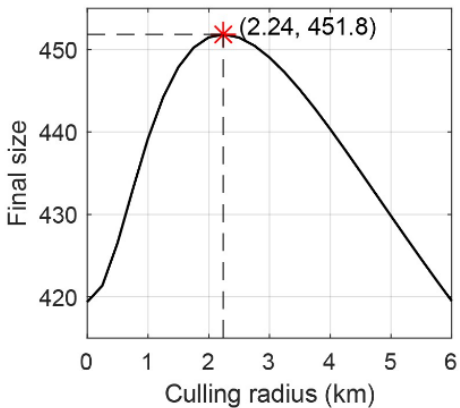


Fig 5. Impact of culling radius on the AI outbreak using the metapopulation model (Eq (2)) with all other parameters in Table 2. The left panel depicts the final size of susceptible farms with respect to culling radius. The right panel displays the total number of PE culling (dot-dashed), IP culling (dashed) and both (solid) with respect to culling radius. Note that when culling radius is 2.24 km, the final size of susceptible farms is maximized and the total number of culling is minimized.

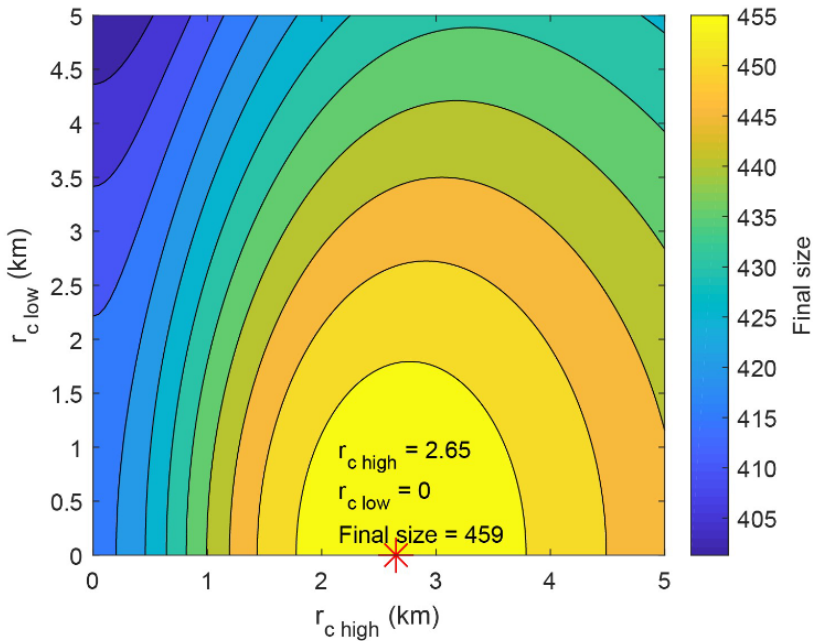


Fig 6. Impact of local-dependent culling radii on the final size of susceptible farms. The final size of susceptible farms with respect to culling radii is maximized as 459 when $r_{c \text{ high}}$ and $r_{c \text{ low}}$ are 2.65 and 0, respectively.

Avian Influenza Spread and Transmission Dynamics*

Lydia Bourouiba

*Department of Mathematics, Massachusetts Institute of Technology,
Cambridge, MA, USA*

Stephen Gourley

Department of Mathematics, University of Surrey, Guildford, Surrey, UK

Rongsong Liu

Department of Mathematics, University of Wyoming, Laramie, WY, USA

John Takekawa

USGS Western Ecological Research Center, Vallejo, CA, USA

Jianhong Wu

Centre for Disease Modelling, York University, Toronto, ON, Canada

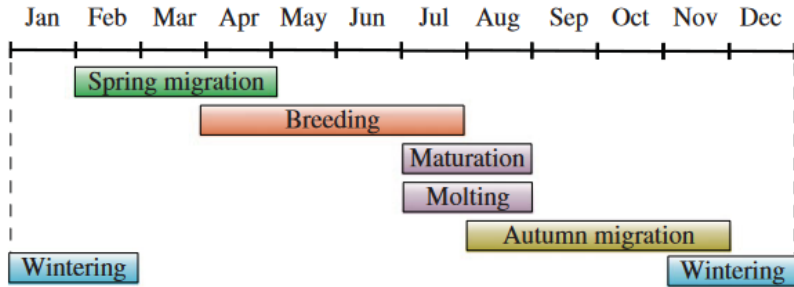


Figure 7.1 Seasonality in migratory and biological functions with overlapping phases

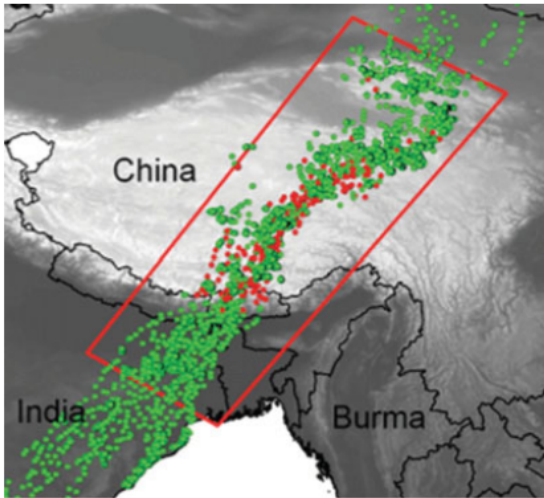


Figure 7.2 Illustration of tracking of Bar-headed geese using GPS locations, showing long-range of motion from India toward Mongolia. Light dots correspond to terrains lower than 5000 meters elevation, while dark dots correspond to terrains higher than 5000 meters elevation (Hawkes et al. 2013)

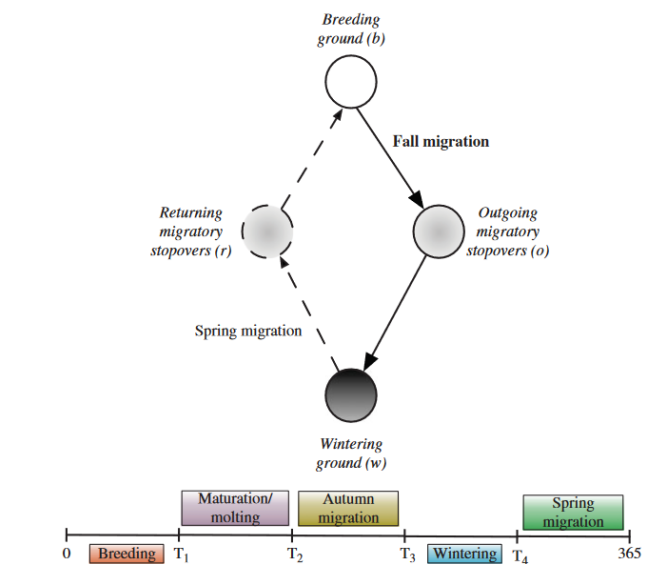


Figure 7.3 Schematic diagram for (top) the spatial dynamics of bird migration in the form of a patch model; and (bottom) the associated temporal dynamics, assuming disjoint phases of bird ecology. In (top), the four patches are labeled *b*, *o*, *w*, *r* for the breeding patch, the outgoing (fall) stopover patch, the wintering patch, and the returning (spring) stopover patch, respectively. The breeding patch is that on which migratory birds breed and mature/molts, while the wintering patch is where they spend the winter season.

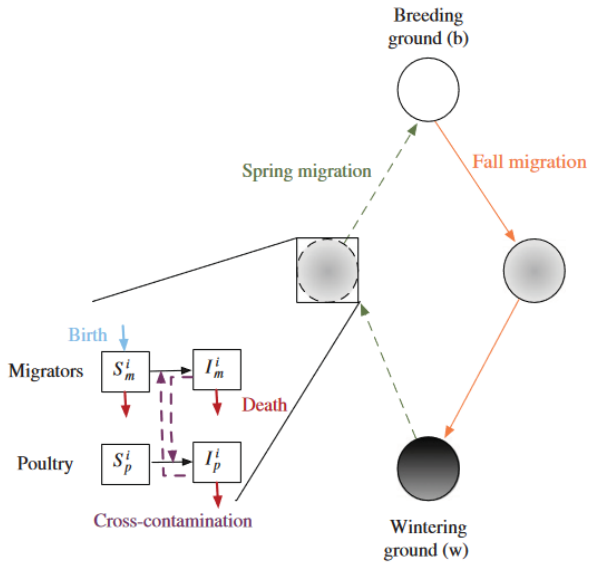


Figure 7.7 Illustration of the multi-scale modeling of disease dynamics. The local disease transmission dynamics and interaction between local poultry and migrators is embedded in the overall cycle of migration, thus, contributing to the global disease pattern. On a given patch i S_m^i and I_m^i are the number of susceptible and infectious migratory birds, respectively; S_p^i and I_p^i are the numbers of susceptible and infectious poultry, respectively